AD-A040 673 PENNSYLVANIA STATE UNIV UNIVERSITY PARK APPLIED RESE--ETC F/G 20/4
FULLY CAVITATING HYDROFOIL RESPONSE TO STREAMWISE SINUSOIDAL AN--ETC(U)
JUN 74 B R PARKIN N00017-73-C-1418

UNCLASSIFIED TM-74-172 NL

1 OF 1
AD A040673

END

DATE FILMED
7-77

(2) B.S.

(6) FULLY CAVITATING HYDROFOIL RESPONSE TO STREAMWISE SINUSOIDAL AND SHARP-EDGED GUSTS AT ZERO CAVITATION NUMBER.

(10) Blaine B. R. Parkin

(11) 4 Jun 74

(12) 46 p.

(9) Technical Memorandum

(14) File No. TM-74-172
June 4, 1974
(15) Contract No. N00017-73-C-1418

Copy No. 38

(16) F43421

(17) ZF4342100 1

The Pennsylvania State University
Institute for Science and Engineering
APPLIED RESEARCH LABORATORY
Post Office Box 30
State College, PA 16801

NAVY DEPARTMENT

NAVAL ORDNANCE SYSTEMS COMMAND

1473

391 007

JB

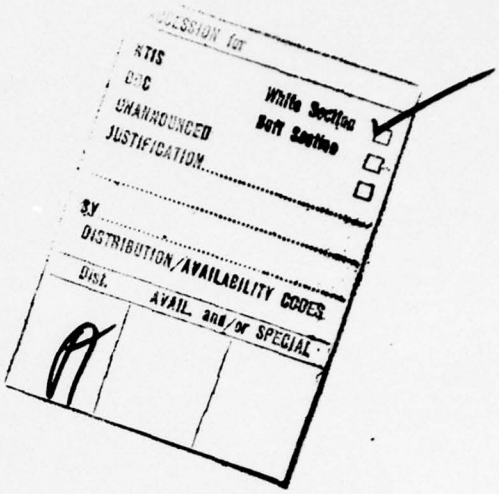

Subject: Fully Cavitating Hydrofoil Response to Streamwise Sinusoidal and Sharp-Edged Gusts at Zero Cavitation Number

References: See Page 32

Abstract: A second-order linearized theory of two-dimensional cavity flows is used to study the nonsteady response of hydrofoil lift and moment to sinusoidal and sharp-edged streamwise gusts. These gust patterns are assumed to be frozen and to be convected at the steady free-stream velocity. The analysis is restricted to the case of zero cavitation number corresponding to an infinitely long cavity in an otherwise unbounded flow. For sinusoidal gusts, lift and moment response functions are presented for the entire range of reduced frequency. In addition, transient lift and moment responses are tabulated for the reactions which occur after the foil encounters a sharp-edged gust. These calculations are carried out for those terms in the solution which result from the nonsteady downwash on the wetted surface of the foil which are due to the direct action of the gust on the inclined wetted surface. They provide a direct cavity flow analog of the Horlock function of airfoil theory. The present study of a cavity flow has revealed an added nonsteady effect resulting from an interaction between the gust and the cavity. Theoretical results for this part of the solution are presented in this report which show a response at twice the input frequency of a sinusoidal gust. Numerical evaluation of this part of the theory has not been carried out.

Acknowledgment: This work was supported by the Naval Material Command under Program Element 62754N, Task Area ZF 43 421 001, administered by the Naval Ship Research and Development Center. This work was performed under Contract Number N00017-73-C-1418.

TABLE OF CONTENTS

INTRODUCTION

The present study is motivated by recent demonstrations that accurate analyses of nonsteady blade forces caused by inflow distortions upstream of propellers [1,2]*and axial-flow turbomachines [3,4] depend upon the streamwise, as well as the transverse, component of gust velocity relative to the blade. In these experimental and theoretical studies, which involve noncavitating flows, the inclusion of the streamwise gust component has been found essential for prediction of nonsteady force trends with advance ratio. Another reason for the present analysis is the current interest in high-speed hydrofoil boats with supercavitating foils. In such craft, the forces on supercavitating propeller blades or ocean wave effects on the foil loads might also depend on the streamwise, as well as the transverse, component of gust velocity. Finally, the possibility that streamwise gusts might also be generated in the course of nonsteady cavity-flow experiments in water tunnels is another reason for considering this problem.

The present study is only a start in the analysis of the nonsteady cavity flow problems noted above. With respect to the first, the effects of neighboring blades are not considered, with respect to the second, the presence of the free surface is neglected, and with respect to the third, the effect of tunnel walls has not been included. The aim here is to obtain the cavity-flow analog of the Horlock function [5] for nonsteady cavity flows, and from this new result to derive nonsteady response functions for lift and moment to sharp-edged gusts. The entire analysis is restricted to two-dimensional flows at zero cavitation number. In this case, the cavity length is infinite. The linearized theory of cavity flows is used to obtain the desired results.

As is also true of Horlock's analysis [5], the nonsteady response of streamwise gusts in cavity flows is a second-order effect. Therefore, the present analysis centers around the systematic development of first, and then second, order approximations. As is convenient in linearized analyses of such nonsteady cavity flows, the acceleration potential is employed. The method of the present study follows an analogous treatment of nonsteady airfoil theory [6]. However, the presence of the long cavity in the hydrofoil case brings certain aspects to the theory which require that we reformulate the analysis from the beginning.

FLOW GEOMETRY AND BASIC EQUATIONS

We shall consider a two-dimensional flat-plate hydrofoil of chord length s at an attack angle $\varepsilon\alpha$ with respect to the free-stream flow direction. The cavity springs from the nose and tail of the profile, and it extends to infinity in the downstream direction. Only the underside of the foil is wetted by the flow, and this surface lies along the x axis. Figure 1 shows the general features of the flow geometry with respect to x-y coordinates. The free-stream velocity, $\vec{q}_\infty$, in Figure 1 includes the sinusoidal gust, $Uw(x,t)$, which is superimposed on the free-stream velocity U. The gust velocity is the only time-dependent input disturbance to an otherwise steady flow. The attack angle $\varepsilon\alpha$ is fixed, and the pressure inside the cavity is constant and equal to the free-stream static pressure, P_o. The quantity ε characterizes the magnitude of all disturbances imposed upon the free-stream flow.

The velocity at any point in the flow, $\vec{q}(x,y,t)$, has two components

*Numbers in parentheses refer to documents given in the list of references.

$$q_x = U(\cos\varepsilon\alpha + w_x + u)$$

and (1)

$$q_y = U(\sin\varepsilon\alpha + w_y + v) \quad .$$

Each of these has a steady free-stream part, the periodic gust, and a disturbance component created by the foil and cavity. The disturbances u and v vanish far from the foil. Moreover, the static pressure at any point in the flow is P(x,y,t). It can be represented as the sum of the constant free-stream pressure P_o, and a disturbance pressure p(x,y,t) created by the foil. Thus,

$$P(x,y,t) = P_o + p(x,y,t) \quad . \tag{2}$$

The disturbance p(x,y,t) also vanishes at points far from the foil and on the cavity.

For an incompressible fluid having density ρ, conservation of momentum requires that

$$\frac{\partial \vec{q}}{\partial t} + (\vec{q}\cdot\nabla)\vec{q} = -\frac{\nabla P}{\rho} \quad . \tag{3}$$

Conservation of mass provides that

$$\text{div } \vec{q} = 0 \quad . \tag{4}$$

If the flow is irrotational,

$$\text{curl } \vec{q} = 0 \quad . \tag{5}$$

In a two-dimensional flow, Equations (4) and (5) imply that a gust in the x-direction should be associated with one in the y-direction. In nonsteady airfoil theory, the response to a constant amplitude vertical sinusoidal gust is given by the well-known Sears' function [7]. The response to a similar streamwise gust has been determined by Horlock [5], with a further extension and interpretation given by Morfey [8]. Commerford and Carta [9] have studied more general two-dimensional sinusoidal transverse and chordwise gusts when the conditions of irrotationality and continuity are explicitly satisfied. They find that gusts of constant amplitude, independent of y, are not strictly permissible. Both components should show transverse amplitude variations represented by multiplicative factors of the form $\exp(\pm\omega y/U)$. They also find that the phase of the horizontal gust leads that of the vertical gust by 90 degrees. The neglect of these conditions in analyses by Sears, Horlock and others appears to be justified by the fact that small vorticity in the flow

does not affect the lift on a thin airfoil. Evidently, independent analyses of constant amplitude vertical and horizontal gust response can provide practically meaningful results. Appropriate combinations of such transverse and horizontal gust response functions can then be used to approximate the response to practical situations [5].

PERTURBATION EQUATIONS

The effect of the gust will be studied under the assumption that the hydrofoil and its cavity are equivalent to a slender body so that disturbances created by the foil will be much smaller than the free-stream velocity U. The parameter ε will be used to characterize the magnitude of all disturbances. In the case of the gust, the chordwise component which is parallel to the wetted surface of the flat plate foil is the interesting quantity. We will specify it by

$$w_x = \varepsilon w_1 = \varepsilon u_o e^{j\omega(t - \frac{x}{U})} \quad , \tag{6}$$

where the constant u_o is the chordwise gust amplitude, ω is the circular frequency, t is the time and $j = \sqrt{-1}$. It follows that

$$w_y = \varepsilon w_1 \tan\varepsilon\alpha = \varepsilon^2 \alpha w_1 + \ldots \quad . \tag{7}$$

It may be remarked that if w_x is not at least of first order in ε, it follows from the continuity condition that it must be zero, which is contrary to hypothesis.

Now, let disturbances created by the foil be represented as

$$\left.\begin{aligned} u &= \varepsilon u_1 + \varepsilon^2 u_2 + \ldots \quad , \\ v &= \varepsilon v_1 + \varepsilon^2 v_2 + \ldots \quad , \\ \text{and} \quad p &= \varepsilon p_1 + \varepsilon^2 p_2 + \ldots \quad . \end{aligned}\right\} \tag{8}$$

Expanding the trignometric functions in Equations (1) in powers of ε and using Equations (6), (7) and (8) in Equations (1), one gets the component velocities,

$$\left.\begin{aligned} q_x &= U\left[1 + \varepsilon(u_1 + w_1) + \varepsilon^2\left(u_2 - \frac{\alpha^2}{2}\right) + \ldots\right] \quad , \\ \text{and} \quad q_y &= U\left[\varepsilon\left(\alpha + v_1\right) + \varepsilon^2\left(v_2 + \alpha w_1\right) + \ldots\right] \quad . \end{aligned}\right\} \tag{9}$$

Now, let us substitute Equations (9) into the irrotationality condition of Equation (5). Then, group all terms according to the power of ε multiplying the terms of each group. Since curl $\vec{q} = 0$ for all admissible values of ε, it follows that

$$\left.\begin{aligned} &\frac{\partial u_1}{\partial y} - \frac{\partial v_1}{\partial x} = 0 \\ \text{and} \quad &\frac{\partial u_2}{\partial y} - \frac{\partial}{\partial x}(v_2 + \alpha w_1) = 0 \quad . \end{aligned}\right\} \tag{10}$$

Similarly, the continuity equation, Equation (4), becomes

$$\left.\begin{aligned} &\frac{\partial}{\partial x}(u_1 + w_1) + \frac{\partial v_1}{\partial y} = 0 \\ \text{and} \quad &\frac{\partial u_2}{\partial x} + \frac{\partial v_2}{\partial y} = 0 \quad . \end{aligned}\right\} \tag{11}$$

The same process applied to the equations of motion also leads to pairs of first order and second order equations.

First Order Equations

$$\left.\begin{aligned} &\frac{1}{U}\frac{\partial u_1}{\partial t} + \frac{\partial u_1}{\partial x} = -\frac{1}{\rho U^2}\frac{\partial p_1}{\partial x} \quad , \\ &\frac{1}{U}\frac{\partial v_1}{\partial t} + \frac{\partial v_1}{\partial x} = -\frac{1}{\rho U^2}\frac{\partial p_1}{\partial y} \quad . \end{aligned}\right\} \tag{12}$$

The gust velocity, because of its form, has zero linearized total derivative, and it does not appear in Equations (12). Moreover, when the first of Equations (11) is combined with the sum of Equations (12), after the first is differentiated with respect to x, and the second with respect to y, one finds that

$$\left(\frac{1}{U}\frac{\partial}{\partial t} + \frac{\partial}{\partial x}\right)\frac{\partial w_1}{\partial x} = \frac{1}{\rho U^2}\nabla^2 p_1 = 0 \quad ,$$

again, because $w_1 = u_o e^{j\omega(t - x/U)}$. Therefore, we can define a harmonic function ϕ_1 such that the gradient of this acceleration potential gives the disturbance acceleration created by the foil:

$$\vec{a}_1 = \nabla\phi_1 \quad .$$

Since $p = p_1 = 0$ at upstream infinity, it also follows that one can put

$$\phi_1 = -\frac{1}{\rho U^2} p_1 \quad . \tag{13}$$

Finally, because $\phi_1(x,y,t)$ is harmonic at every instant, one can use the Cauchy-Riemann equations to define a conjugate function $\psi_1(x,y,t)$:

$$\left.\begin{aligned} \frac{\partial\phi_1}{\partial x} = \frac{\partial\psi_1}{\partial y} = a_{x_1} \quad , \\ \frac{\partial\phi_1}{\partial y} = -\frac{\partial\psi_1}{\partial x} = a_{y_1} \quad . \end{aligned}\right\} \tag{14}$$

As a result, a complex acceleration potential can be defined as $F_1 = \phi_1 + i\psi_1$ and a complex velocity by $W_1 = u_1 - iv_1$, where $i = \sqrt{-1}$ and $ij \neq -1$. It follows that the complex sum of Equations (11) can be written in terms of two analytic functions of $z = x + iy$ as

$$\frac{1}{U}\frac{\partial W_1}{\partial t} + \frac{dW_1}{dz} = \frac{dF_1}{dz} \quad . \tag{15}$$

Second Order Equations

Upon separating the second order terms from the equations of motion and using the first order irrotationality condition to transform certain convective terms, one finds that

$$\left.\begin{aligned} \frac{1}{U}\frac{\partial u_2}{\partial t} + \frac{\partial u_2}{\partial x} = -\frac{\partial}{\partial x}\left\{\frac{p_2}{\rho U^2} + \frac{(w_1 + u_1)^2 + (v_1 + \alpha)^2}{2}\right\} \\ \text{and} \\ \frac{1}{U}\frac{\partial v_2}{\partial t} + \frac{\partial v_2}{\partial x} = -\frac{\partial}{\partial y}\left\{\frac{p_2}{U^2} + \frac{(w_1 + u_1)^2 + (v_1 + \alpha)^2}{2}\right\} \quad . \end{aligned}\right\} \tag{16}$$

Again, differentiation of the first member of this pair with respect to x, and the second with respect to y and use of the second order continuity equation, leads to

$$\nabla^2 \left\{ \frac{p_2}{\rho U^2} + \frac{(w_1 + u_1)^2 + (v_1 + \alpha)^2}{2} \right\} = 0 \quad .$$

As before, we set

$$\nabla \phi_2 = - \nabla \left\{ \frac{p_2}{\rho U^2} + \frac{(w_1 + u_1)^2 + (v_1 + \alpha)^2}{2} \right\} .$$

The integral of this equation is

$$\phi_2 + \frac{p_2}{\rho U^2} + \frac{(w_1 + u_1)^2 + (v_1 + \alpha)^2}{2} = f(t) \quad .$$

When $u_o = 0$ the flow must become steady and so $f(t)$ is a constant which we will put equal to zero. At upstream infinity, $p_2 = u_1 = v_1 = 0$, and since the value of ϕ_2 is at our disposal there, we will put $\phi_2(-\infty) = - (w_1^2+\alpha^2)/2$. As will be seen below, this choice of $\phi_2(-\infty)$ insures that p_2 is zero on the trailing edge of the foil, and of greater importance, that ϕ_2 is also zero at the trailing edge. Had we chosen $\phi_2(\infty,t) = 0$, the value of p_2 would still be zero at the trailing edge, but ϕ_2 would have been equal to $\alpha^2/2$ there. The present choice is, therefore, the more convenient one. From these considerations it follows that

$$\phi_2 = - \left[\frac{p_2}{\rho U^2} + \frac{(w_1 + u_1)^2 + (v_1 + \alpha)^2}{2} \right] \quad . \tag{17}$$

In Equation (17) the term w_1^2 is bounded but not well behaved at $z = -\infty$. However, it leads to no second-order acceleration components anywhere in the flow. Its effect will be treated separately below.

Clearly, $\nabla^2 \phi_2 = 0$ and the acceleration components can be expressed in terms of the Cauchy-Riemann equations as

$$a_{x_2} = \frac{\partial \phi_2}{\partial x} = \frac{\partial \psi_2}{\partial y} \quad ,$$

$$a_{y_2} = \frac{\partial \phi_2}{\partial y} = - \frac{\partial \psi_2}{\partial x} \quad .$$

As was the case for the first order system, one can define a complex acceleration potential

$$F_2 = \phi_2 + i\psi_2 \quad .$$

In the limit of steady flow, the first of Equations (16) becomes

$$\frac{\partial u_2}{\partial x} = \frac{\partial \phi_2}{\partial x}$$

and if one integrates from $z = -\infty$ to $z = x$, he gets

$$\phi_{2\ \text{steady}} = u_2 - \frac{\alpha^2}{2} \quad .$$

The second of Equations (16) becomes

$$\psi_{2\ \text{steady}} = - v_2 \quad .$$

BOUNDARY CONDITIONS

The solution of the present problem depends upon the determination of an analytic function

$$F(z,t;\varepsilon) = \varepsilon F_1 + \varepsilon^2 F_2 + \ldots \quad , \tag{18}$$

which at each instant is regular outside the foil and the cavity. The complex potential F will satisfy certain boundary conditions, which in keeping with thin-body approximations are transferred to a cut along the positive real axis of the z plane. This mathematical representation of the foil and the cavity is illustrated in Figure 2.

As noted previously, the wetted surface of the foil is positioned on the real axis ($0 \leq x \leq s$, $y = 0-$). We shall denote the cavity contour by $y = \varepsilon C_{\pm}(x)$, where C_+ and C_- refer to the upper or the lower contours, respectively. The boundary conditions which apply in the z plane are:

(i) $p(x,y,t) = 0$ for $0 \leq x$, $y = \varepsilon C_+(x)$; $s \leq x$, $y = \varepsilon C_-(x)$.

(ii) $F(z)$ continuous at $x = s$, $y = 0-$ (Kutta Condition).

(iii) $F(z) = -\varepsilon^2(w_1^2 + \alpha^2)/2$ at $z = -\infty$ [because of Equation (17)]

(iv) $q_y = 0$ for $0 \leq x \leq s$, $y = 0-$.

Finally, if v_f is the downwash on the wetted surface of the foil, the vertical acceleration of the fluid there, is

(v) $\left(\frac{1}{U}\frac{\partial}{\partial t} + \frac{\partial}{\partial x}\right) v_f = a_{y_f}$; $0 \leq x \leq s$, $y = 0-$.

These boundary conditions can now be separated into first and second order systems with the help of Equations (8), (9), (11), (17), and (18). In order to carry out this separation for (i), the conditions must be transferred from the cavity contours to the top or bottom of the cut along the real axis. This step is carried out by using a MacLaurin's series in $y = \varepsilon C_{\pm}$:

$$p_n = p_n\,(x,0\pm,t) + \varepsilon C_{\pm}(x)\,\frac{\partial}{\partial y}\,p_n\,(x,0-,t) + \ldots\,,\quad n = 1,2\ .$$

The first and second order boundary conditions take the following forms.

First Order

I(i) $\quad \mathrm{Re}\,\{F_1(x,0,t)\} = 0,\ 0 \leq x,\ y = 0+\ ;\ s \leq x,\ y = 0-$.

I(ii) $\quad F_1(z,t)$ continuous at $x = s$, $y = 0-$ (Kutta Condition) .

I(iii) $\quad F_1(-\infty,t) = 0$.

I(iv) $\quad v_1(x,0-,t) = -\alpha\ ,\ 0 \leq x \leq s$.

Evidentally, these conditions indicate a steady flow for the first order solution, so that $F_1 = W_1$, or $\phi_1 = u_1(x,y)$, $\psi_1 = -v_1(x,y)$. It is to be noted that I(iv) guarantees the satisfaction of condition (v) above.

Second Order

II(i) $\quad \mathrm{Re}\,\{F_2(z,t)\} = -C_{\pm}\,\dfrac{\partial v_1}{\partial x} - \dfrac{w_1^2 + (v_1 + \alpha)^2}{2}\ ;\ x \geq \begin{Bmatrix} 0 \\ s \end{Bmatrix},\ y = \begin{Bmatrix} 0+ \\ 0- \end{Bmatrix}$.

II(ii) $\quad F_2(z,t)$ continuous at $x = s$, $y = 0-$.

II(iii) $$F_2(z,t) = -\frac{w_1^2 + \alpha^2}{2} \text{ at } z = -\infty \quad .$$

II(iv) $$v_2 = -\alpha\, w_1;\ 0 \leq x \leq s,\ y = 0- \quad .$$

II(v) $$\text{Im}\left\{\frac{dF_2}{dz}\right\} = 0,\ 0 \leq x \leq s,\ y = 0- \quad .$$

In the first of these conditions, the first order result $\psi_1 = -v_1$ and cavity pressure condition $u_1 = 0$ have been used. As a result, II(i) becomes $\phi_2 = -w_1^2/2$ on the lower surface of the cavity at the trailing edge because $v_1 = -\alpha$ and $C_- = 0$ there. But, since ϕ_2 is continuous at the trailing edge, it follows from Equation (17) that $p_2 = 0$ there. The foregoing basic equations and boundary conditions permit us to attack the first and second order problems.

FIRST ORDER SOLUTION

Although the first order solution is a well-known result of linearized cavity flow theory, it will be reviewed in this section because the second order solution requires specific first order results and the theoretical approach to the first order problem is also useful in the second order case. In the following, a sequence of conformal mappings will be used. The region outside the wetted surface of the foil and the cavity, represented by the cut along the positive real axis in the z-plane, Figure 2, is transformed into the region above the real axis and the unit semicircle about the origin in the ζ-plane. This result is achieved by first mapping the region outside the cut in the z-plane into the upper half of the ν-plane by means of a square-root relationship. Then that part of the real ν-axis corresponding to the wetted surface of the foil is mapped into the upper half of the unit circle in the ζ-plane by means of a Joukowski transformation. Thus, one can write for both first and second order flows,

$$\sqrt{\frac{z}{s}} = \nu = \frac{1}{4}\left(\zeta + \frac{1}{\zeta}\right) - \frac{1}{2} \quad . \tag{19}$$

The ν- and ζ-planes with corresponding points on the cavity and foil are shown in Figures 3 and 4. In these mappings the complex acceleration potential $F(z,t;\varepsilon)$ is invariant at corresponding points.

As already noted, the first order flow is steady and $F_1 = W_1 = u_1 - iv_1$. In the ζ-plane, an analytic function which satisfies the boundary conditions I(i) through 1(iv) can be found by inspection This function is

$$f = \frac{i}{\zeta - 1} \quad .$$

It can be seen that f is purely imaginary when ζ is any point on the real axis. Evidentally, f satisfies I(i). This function has a leading edge singularity

which provides for the branching of the flow at the nose of the hydrofoil. At $\zeta = 1$, changes in velocity must be of the same order as the free-stream velocity so that the small-disturbance assumptions of the theory break down in the neighborhood of the nose. On the other hand, it is certainly clear that the Kutta condition I(ii) is satisfied at the trailing edge, $\zeta = -1$. In fact, Re f = 0 there. Moreover, as can be seen from Equation (19), large values of $|\zeta|$ correspond to large values of $|z|$. Therefore I(iii) is certainly satisfied. Finally, at points on the wetted surface of the foil $\zeta = e^{i\theta}$ and $2f = \cot\theta/2 - i$. Accordingly, f can also be made to satisfy I(iv) if we put f equal to

$$F_1 = W_1(z) = \frac{-2i\alpha}{\zeta - 1} \tag{20}$$

One can use Equation (19) for corresponding points on the profile, for which $\zeta = e^{i\theta}$ and $\sqrt{z/s} = -\sqrt{x/s}$, to show that $\cos\theta = 1 - 2\sqrt{x/s}$. It then follows from Equation (20) that

$$\left.\begin{aligned} u_1 &= -\alpha\sqrt{\sqrt{\frac{s}{x}} - 1} \\ \text{and} \qquad v_1 &= -\alpha \end{aligned}\right\} \tag{21}$$

on the wetted surface of the foil. From Equation (13), it follows for steady flow that $u_1 = -p_1/\rho U^2$, or that $C_{p_1} = -2u_1$. One can integrate the pressure coefficient along the wetted surface of the foil to find expressions for the section force coefficients. For example, the section lift coefficient, C_{ℓ_1}, is

$$C_{\ell_1} = 2\alpha \int_0^1 \sqrt{\sqrt{\frac{s}{x}} - 1}\, d\left(\frac{x}{s}\right) = \frac{\pi}{2}\alpha \quad . \tag{22}$$

Similarly, the section moment coefficient about the profile nose is,

$$C_{m_1} = 2\alpha \int_0^1 \left(\frac{x}{s}\right)\sqrt{\sqrt{\frac{s}{x}} - 1}\, d\left(\frac{x}{s}\right) = -\frac{5\pi}{32}\alpha \quad . \tag{23}$$

Nose-up moments are positive. Because the wetted surface of the profile is flat, the cavity drag coefficient for the section is

$$C_{d_1} = \alpha\, C_{\ell_1} = \frac{\pi}{2}\alpha^2 \quad .$$

One can also write specific expressions for the cavity contours $C_{\pm}(x)$. However, these expressions will not be needed for the nonsteady solution, and we can omit this detail.

DISCUSSION OF SECOND ORDER BOUNDARY CONDITIONS

The boundary conditions for the second order solution as defined by the five conditions II can be split into uncoupled steady and nonsteady parts. For the steady part we have:

Steady Boundary Conditions

(i) $$u_2 - \frac{\alpha^2}{2} = - C_{\pm} \frac{\partial v_1}{\partial x} - \frac{(v_1 + \alpha)^2}{2} \quad , \quad y = \left\{ \begin{matrix} 0+ \\ 0- \end{matrix} \right\} \quad , \quad x \geq \left\{ \begin{matrix} 0 \\ s \end{matrix} \right\}$$

(ii) $W_2(z)$ continuous at $x = s$, $y = 0-$.

(iii) $\phi_2 = - \frac{\alpha^2}{2}$ at $z = -\infty$ (and $u_2 = v_2 = 0$ there).

(iv) $v_2 = 0$, $0 \leq x \leq s$, $y = 0-$.

If allowance is made for the somewhat different notation used here, and the fact that we consider the special case of the flat plate profile, it can be seen that these conditions correspond to those given by Chen [10]. In view of Chen's results, we need not consider the steady problem. We can proceed directly to the study of nonsteady gusts.

Nonsteady Boundary Conditions

(i) $$\text{Re}\{F_2(z,t)\} = - \frac{w_1^2}{2} \; ; \; x \geq \left\{ \begin{matrix} 0 \\ s \end{matrix} \right\} \quad , \quad y = \left\{ \begin{matrix} 0+ \\ 0- \end{matrix} \right\} \quad .$$

(ii) $F_2(z,t)$ continuous at $x = s$, $y = 0-$.

(iii) $a_x = a_y = 0$ at $x = -\infty$.

(iv) $v_2 = -\alpha w_1$; $0 \leq x \leq s$, $y = 0-$.

(v) $$\text{Im} \left\{ \frac{dF_2}{dz} \right\} = 0; \; 0 \leq x \leq s, \; y = 0- \quad .$$

Inspection of the five nonsteady boundary conditions listed above reveals that (i) and (iv) have different behavior with respect to the gust frequency as indicated by the power of w_1 which occurs in each one of these expressions. In particular, (i) shows the doubled frequency dependence of 2ω and (iv) depends on ω only. In order to handle this situation we shall let the solution

be the sum of two parts: $F_2(z;\omega) + \tilde{F}_2(z;2\omega)$. The first part accounts for the nonsteady downwash generated on the wetted surface of the foil and the second part concerns the interaction between gust and cavity. Then we can split the nonsteady boundary conditions by writing the boundary conditions for $F_2(z;\omega)$ so that its condition (i) reads

$$\text{Re}\,\{F_2(z;\omega)\} = 0 \;;\; x \geq \begin{Bmatrix} 0 \\ s \end{Bmatrix}, \; y = \begin{Bmatrix} 0+ \\ 0- \end{Bmatrix},$$

with all others remaining as written above. For the case of $\tilde{F}_2(z;2\omega)$ we will write condition (iv) to read

$$\tilde{v}_2 = 0 \;;\; 0 \leq x \leq s \;,\; y = 0-$$

with all others remaining as written above. In this latter case we note that if this homogeneous streamline condition is satisfied on the wetted surface, then the homogeneous condition (v) for the acceleration, $\text{Im}\,\{dF_2(z;2\omega)/dz\} = 0$ will be satisfied identically at points on the foil. However if the acceleration condition is satisfied first, one must still see to it that the streamline condition on $\tilde{v}_2$ is satisfied explicitly.

We will now turn to the determination of the function $F_2(z;\omega)$, which accounts for the nonsteady downwash on the foil and which, as we shall see, leads to the direct cavity-flow analog of the Horlock function, $T(\omega)$.

THE ANALOG OF HORLOCK'S FUNCTION

As we have noted above, the boundary conditions for $F_2(z;\omega)$ are:

(i) $\text{Re}\,\{F_2(z;\omega)\} = 0 \;;\; x \geq \begin{Bmatrix} 0 \\ s \end{Bmatrix}, \; y = \begin{Bmatrix} 0+ \\ 0- \end{Bmatrix}$.

(ii) $F_2(z;\omega)$ continuous at $x = s$, $y = 0-$.

(iii) $F_2(-\infty;\omega) = 0$.

(iv) $v_2 = -\alpha\, w_1 \;;\; 0 \leq x \leq s \;,\; y = 0-$.

(v) $\text{Im}\,\{dF_2(z;\omega)/dz\} = 0 \;;\; 0 \leq x \leq s \;,\; y = 0-$.

Having "suppressed" the term w_1^2 in these conditions, we must also suppress the corresponding term in Equation (17). Thus, for this part of the nonsteady solution Equation (17) is replaced by

$$\phi_2 = -\left[\frac{p_2}{\rho U^2} + \frac{u_1^2 + (v_1 + \alpha)^2}{2} + u_1 w_1\right] \quad . \tag{17a}$$

Thus, ϕ_2 for this case will show no frequency doubling.

Comparison of these nonsteady second order conditions on $F_2(z;\omega)$ with the first order conditions considered previously suggests that the function f, introduced for the first order solution, should be adaptable to the nonsteady problem. Condition (iv) will lead to some differences in the method of solution, but it is clear that the present conditions (i), (ii), and (iii) are satisfied by f. It can also be seen that condition (v) is also satisfied by f. One can verify this by using the fact that in the ζ-plane, the real and imaginary parts of the product $e^{i\theta}df/d\zeta$ give the radial and transverse components of acceleration. By using this relationship, one can verify that f produces no radial component of acceleration on the unit circle. Therefore, this function produces no acceleration component a_y on the wetted surface in the z-plane, except possibly at the leading edge where f is singular. In order to adapt f to the present situation, we will introduce a function

$$A(t) = A_o e^{j\omega t} \quad . \tag{24}$$

The factor $A_o(\omega)$ will be determined by condition (iv). The time dependence is separated out as indicated in Equation (24) because w_1, as defined in Equation (6), can also be separated in this way. Thus, we shall write the nonsteady solution as

$$F_2(\zeta,t) = \frac{iA_o e^{j\omega t}}{\zeta - 1} \quad . \tag{25}$$

In order to determine the quantity A_o and, thus, complete the solution of Equation (25), it is necessary to satisfy nonsteady condition (iv) by integrating the second of Equations (16)*. Again, we separate the spatial and temporal factors by writing $v_2 = v_o(x,y)e^{j\omega t}$ and $\psi_2 = \psi_o(x,y)e^{j\omega t}$ to obtain

$$j\frac{\omega}{U} v_o + \frac{\partial v_o}{\partial x} = -\frac{\partial \psi_o}{\partial x} \quad . \tag{26}$$

This equation can now be integrated from $x = -\infty$ along the negative real axis to a point near or on the wetted surface of the foil. Introducing the reduced frequency,

*Note that now the term w_1^2 is suppressed as indicated in Equation (17a).

$$k \equiv \frac{\omega s}{U} \quad ,$$

based on the entire profile chord length, one can write

$$v_o = - e^{-jk\frac{x}{s}} \int_{-\infty}^{x} \frac{\partial \psi_2}{\partial x} e^{jk\frac{\xi}{s}} d\xi \qquad (28)$$

for the integral of Equation (26). Assuming that this integral is convergent, one can consider x to be a point on the wetted surface and he can differentiate both sides of Equation (28) with respect to x. But on the foil, nonsteady condition (v) indicates that $\partial\psi_o/\partial_x = 0$ there. Therefore, it also follows that $\partial v_o/\partial x = - (jk/s)v_o$ on the wetted surface. Moreover condition (iv) indicates that $v_o = - \alpha u_o \exp(-jkx/s)$ when $0 < x \leq s$, $y = 0-$. Therefore Equation (28) is identically satisfied at all points on the wetted surface of the profile. This fact permits us to take $x = 0+$ in Equation (28) without loss of generality. However, in order to secure convergence in the evaluation of Equation (28), we integrate by parts. We take the principal value of the integral by indenting the contour of integration by means of a small semicircle about the nose in the lower half z-plane. Thus, the path of integration goes from $-\infty$ to $\varepsilon e^{i\pi}$ and then around the semicircle from $\varepsilon e^{i\pi}$ to $\varepsilon e^{i2\pi}$. Finally, one takes the limit $\varepsilon \to 0$. Thus, Equation (28) becomes

$$- \alpha u_o = - \psi_o(0+) + jk \int_{0-}^{-\infty} e^{jk\frac{x}{s}} \psi_o \left(\frac{x}{s}\right) d\left(\frac{x}{s}\right) \quad . \qquad (29)$$

From Equation (25) one finds that $\psi_o(0+) = - A_o/2$ and that

$$\psi_o(xe^{\pi i}) = \frac{A_o}{2} \left\{ - 1 + \sqrt{\frac{1 + \sqrt{1 + \left|\frac{s}{x}\right|}}{2}} \right\} \quad .$$

Now, one can put $x/s = - \eta$ and substitute the above relationships into Equation (29) to obtain

$$- \alpha u_o = \frac{A_o}{2} \left\{ 1 + jk \int_{o}^{\infty} \left[\sqrt{\frac{\sqrt{1 + 1/\eta} + 1}{2}} - 1 \right] e^{-jk\eta} \, d\eta \right\} \quad .$$

Solving for A_o, one finds that

$$A_o = \frac{- 2\alpha \, u_o}{1 + jk \, I_1 \, (k)} \quad ,$$

where the integral I_1 is of obvious definition. The close resemblence of Equation (30) to Martin's [11] result for the transverse sinusoidal gust is noteworthy. In Reference [11], Martin has put

$$L(k) = \frac{1}{1 + jk\, I_1} \tag{31}$$

and noted that L(k) is the cavity-flow analog of the Sears' function. Numerical values of L(k) are tabulated in Reference 12. For values of $k \leq 20$, the integral I_1 was evaluated by numerical integration [13]. For calculations involving reduced frequencies exceeding 20, the quantity $1 + jkI_1$ was approximated by an asymptotic expansion [13].

NONSTEADY FORCE AND MOMENT FOR THE FIRST PART OF THE SOLUTION

The nonsteady hydrodynamic force and moment depend on the quantity ϕ_2 for points on the wetted surface of the hydrofoil. We can separate the time dependence by writing $\phi_2 = \phi_o e^{j\omega t}$ as we have done with other second order quantities. One can use Equations (25), (30) and (31) to express ϕ_o on the wetted surface as

$$\phi_o = -\alpha u_o\, L(k) \sqrt{\sqrt{\frac{s}{x}} - 1} \quad .$$

From Equation (17a) one can write the pressure coefficient on the foil as

$$C_{p_2} = -2\left[\phi_2 + \frac{u_1^2}{2} + u_1 w_1\right] \quad .$$

This expression can be decomposed into a steady part C_{p_2} and a nonsteady part $C_{p_o} e^{j\omega t}$. The steady part,

$$C_{p_2} = -2\left[u_2 - \frac{\alpha^2}{2} + \frac{u_1^2}{2}\right] \quad ,$$

would be used for the steady second-order problem. The nonsteady part,

$$C_{p_o} = -2\left[\phi_o + u_1\, u_o e^{-jk\frac{x}{s}}\right] \quad ,$$

is applicable to the present nonsteady problem. In particular,

$$C_{p_o} = + 2\alpha u_o \left[L(k) + e^{-jk\frac{x}{s}} \right] \sqrt{\sqrt{\frac{s}{x}} - 1} \quad .$$

The unsteady section lift and moment coefficients are obtained by integrating this pressure over the wetted surface of the profile. These integrations give

$$C_\ell = \frac{\pi}{2} \alpha u_o \{L(k) + \frac{4}{\pi} I_2(k)\} e^{j\omega t} = \frac{\pi}{2} \alpha u_o P(k) e^{j\omega t} \tag{32}$$

and

$$C_m = - \frac{5\pi}{32} \alpha u_o \{L(k) + \frac{64}{5\pi} I_3(k)\} e^{j\omega t} = - \frac{5\pi}{32} \alpha u_o Q(k) e^{j\omega t} \tag{33}$$

The bracketed terms represent the ratio of nonsteady to quasi-steady response and they will be denoted by P(k) for the lift ratio and by Q(k) for the moment ratio. The integrals I_2 and I_3 are defined by

$$I_2(k) = \int_o^1 \sqrt{\frac{1}{\sqrt{\eta}} - 1}\, e^{-jk\eta}\, d\eta \tag{34}$$

and

$$I_3(k) = \int_o^1 \sqrt{\frac{1}{\sqrt{\eta}} - 1}\, e^{-jk\eta}\, \eta d\eta \quad . \tag{35}$$

Although these integrals show some similarities to others of hypergeometric form, they are not reducible to standard representations. They must be evaluated numerically.

The integrations for I_2 and I_3 have been carried out numerically as indicated in the Appendix. The results of this work are shown in Figure 5 which is a polar plot of P(k) and Q(k) with selected values of k shown on the curves. Figure 6 compares P(k) with functions of Sears [7] and Horlock [5], referred to the profile nose and with the reduced frequency based on the whole chord. The transverse gust function for cavity flow L(k) [11,12] is also plotted in these graphs. In all of these graphs, it is seen that the steady state limit of P and Q as $k \to 0$ is 2. As pointed out previously by Horlock [5], this doubling is caused by the fact that the gust, being in the direction of flight, affects the dynamic pressure experienced by the foil. But the dynamic pressure depends upon the square of the velocity and this fact is responsible for the limit noted.

The indicial admittance functions corresponding to an encounter of the foil with a sharp-edged gust or unit step in chordwise disturbance velocity can be found by direct superposition [13,16]. For the lift response, one can write

$$A_\ell(\lambda) = \frac{2}{\pi} \int_0^\infty \text{Re } \{P(k)\} \frac{\sin\lambda k}{k} \, dk \quad . \tag{36}$$

For the moment response one has

$$A_m(\lambda) = \frac{2}{\pi} \int_0^\infty \text{Re } \{Q(k)\} \frac{\sin\lambda k}{k} \, dk \quad . \tag{37}$$

Again, numerical integrations are required. An outline of this work is also given in the Appendix. The results are shown in Figure 7 which shows the two admittance functions (36) and (37) plotted against λ. The quantity λ is the distance traveled in chord lengths after the profile nose hits the gust. When these functions are known, the lift and moment coefficients are

$$C_\ell(\lambda) = \frac{\pi}{2} \alpha u_o \, A_\ell(\lambda) \tag{38}$$

and

$$C_m(\lambda) = \frac{5\pi}{32} \alpha u_o \, A_m(\lambda) \quad . \tag{39}$$

NONSTEADY CAVITY-GUST INTERACTIONS

It remains to determine the effect of the term $w_1^2 = u_o^2 e^{2j\omega(t-x/U)}$ on the nonsteady hydrodynamics of the cavity flow. From the previous discussion of the second-order boundary conditions we have seen that the nonsteady effect of w_1^2 is ascribable to that part of the complex acceleration potential, $\tilde{F}_2(z;2\omega)$.

It was noted that the boundary conditions for this function are

(i) $\text{Re } \{\tilde{F}_2\} = -\frac{w_1^2}{2}$; $x \geq \begin{Bmatrix} 0 \\ s \end{Bmatrix}$, $y = \begin{Bmatrix} 0+ \\ 0- \end{Bmatrix}$.

(ii) $\tilde{F}_2$ continuous at $x = s$, $y = 0-$.

(iii) $a_x = a_y = 0$, at $x = -\infty$.

(iv) $\tilde{v}_2 = 0$; $0 \leq x \leq s$, $y = 0-$.

(v) $\text{Im } \{\frac{dF_2}{dz}\} = 0$, $0 \leq x \leq s$, $y = 0-$.

We have also observed that conditions (iv) and (v) are somewhat redundant, but

if one knows that (v) is satisfied by $\tilde{F}_2$ he must still be certain that (iv) is explicitly satisfied. Finally it is to be noted that now

$$\tilde{\phi}_2 = -\left[\frac{\tilde{p}_2}{\rho U^2} + \frac{w_1^2}{2}\right] \quad . \tag{17b}$$

In the following we will introduce the reduced frequency k of Equation (27) and factor the term w_1^2 into spatial and temporal parts so that

$$\frac{w_1^2}{2} = \frac{u_o^2}{2} e^{-2jk\frac{x}{s}} e^{2j\omega t} \quad .$$

The temporal part can then be elliminated from further consideration by writing $\tilde{F}_2 = \tilde{F}e^{2j\omega t}$ and so forth for the other quantities defined above. The boundary values which apply to $F = \tilde{\phi} + i\tilde{\psi}$ in the ν-plane are illustrated in Figure 8.

In the z-plane, the normal acceleration condition on the wetted surface of the foil is $\partial\psi/\partial x = 0$ and this can be integrated along the wetted surface to give

$$\tilde{\psi} = B(k) \text{ on } y = 0-,\ 0 \leq x \leq s \quad . \tag{40}$$

Therefore the values illustrated in Figure 8 in the ν-plane on the real axis can be replaced by

$$\tilde{\phi} = -\frac{u_o^2}{2} e^{-2jk\xi^2} \qquad \text{on the upper and lower surfaces of cavity}$$

and

$$\tilde{\psi} = B(k) \qquad \text{on the wetted surface of the profile.}$$

The constant of integration B(k) will be determined later by applying the condition $\tilde{v} = 0$ on the wetted surface. For the present, one observes that the boundary values for $\tilde{F}$ are now specified along alternate intervals of the ξ-axis in terms of $\tilde{\phi}$ and $\tilde{\psi}$. One can transform this specification into a boundary value problem on just the real part of an analytic function $G(\nu)$ by introducing the transformation,

$$G\sqrt{\frac{\xi+1}{\xi}} = \tilde{F} = \tilde{\phi} + i\tilde{\psi} \quad . \tag{41}$$

For then, we have on the ξ axis:

$$\text{for } \xi < -1 \text{ , } G\sqrt{\frac{|\xi| - 1}{|\xi|}} = \tilde{\phi} + i\tilde{\psi} \rightarrow \text{ReG} = \tilde{\phi}\sqrt{\frac{|\xi|}{|\xi| - 1}} \quad ;$$

$$\text{for } -1 < \xi < 0 \text{ , } iG\sqrt{\frac{1 - |\xi|}{|\xi|}} = \tilde{\phi} + i\tilde{\psi} \rightarrow \text{ReG} = \tilde{\psi}\sqrt{\frac{|\xi|}{1 - |\xi|}} \quad ;$$

$$\text{for } \xi > 0 \text{ , } G\sqrt{\frac{\xi + 1}{\xi}} = \tilde{\phi} + i\tilde{\psi} \rightarrow \text{ReG} = \tilde{\phi}\sqrt{\frac{\xi}{\xi + 1}} \quad .$$

Thus ReG is specified on the entire real axis and ImG can be found on the real axis by use of the Hilbert Transform [15],

$$\text{ImG} = -\frac{1}{\pi} P \int_{-\infty}^{\infty} \frac{\text{ReG}(t)}{t - \xi}\, dt \quad . \tag{42}$$

Substituting appropriate values of ReG into Equation (42) one finds that

$$\text{ImG} = \frac{u_o^2}{2\pi} P \int_{-\infty}^{-1} e^{-2jkt^2} \sqrt{\frac{|t|}{|t| - 1}}\, \frac{dt}{t - \xi} - \frac{B(k)}{\pi} P \int_{-1}^{0} \sqrt{\frac{|t|}{1 - |t|}}\, \frac{dt}{t - \xi}$$

$$+ \frac{u_o^2}{2\pi} P \int_{0}^{\infty} e^{-2jkt^2} \sqrt{\frac{t}{t + 1}}\, \frac{dt}{t - \xi} \quad .$$

If one substitutes the appropriate signed value of $|t|$ in the above integrands and also rearranges the limits of integration he finds, after dropping the absolute value symbol from the dummy of integration, that

$$\text{ImG} = -\frac{u_o^2}{2\pi} P \int_{1}^{\infty} e^{-2jkt^2} \sqrt{\frac{t}{t - 1}}\, \frac{dt}{t + \xi} + \frac{B(k)}{\pi} P \int_{0}^{1} \sqrt{\frac{t}{1 - t}}\, \frac{dt}{t + \xi}$$

$$+ \frac{u_o^2}{2} P \int_{0}^{\infty} e^{-2jkt^2} \sqrt{\frac{t}{t + 1}}\, \frac{dt}{t - \xi} \quad .$$

When ξ is on the wetted surface of the foil $-1 \leq \xi \leq 0$, one can put $\xi = -\eta$ in this last equation and find the principal value of the integral involving B(k) to be

$$P\int_0^1 \sqrt{\frac{t}{1-t}}\,\frac{dt}{t-\eta} = \pi \quad .$$

The remaining integrals are no longer improper for points on the foil and so

$$\mathrm{ImG}(\eta) = B(k) + \frac{u_o^2}{2\pi}\left\{\int_0^\infty e^{-2jkt^2}\sqrt{\frac{t}{t+1}}\,\frac{dt}{t+\eta} - \int_1^\infty e^{-2jkt^2}\sqrt{\frac{t}{t-1}}\,\frac{dt}{t-\eta}\right\} \quad . \tag{43}$$

From Equation (41) one finds for points on the wetted surface, with $0 < \eta < 1$, that

$$\tilde{\phi} + i\tilde{\psi} = -\left(\mathrm{ImG}(\eta)\right)\sqrt{\frac{1-\eta}{\eta}} + i\left(\mathrm{ReG}(\eta)\right)\sqrt{\frac{1-\eta}{\eta}} \quad .$$

Therefore, the acceleration potential on the foil is

$$\tilde{\phi}(\eta,0) = \sqrt{\frac{1-\eta}{\eta}}\left[-B(k) - \frac{u_o^2}{2\pi}\left\{\int_0^\infty e^{-2jkt^2}\sqrt{\frac{t}{t+1}}\,\frac{dt}{t+\eta} - \int_1^\infty e^{-2jkt^2}\sqrt{\frac{t}{t-1}}\,\frac{dt}{t-\eta}\right\}\right] \quad . \tag{44}$$

But the Kutta condition requires that $\tilde{\phi}(1,0;k) = -\frac{u_o^2}{2}e^{-2jk}$ in accordance with conditions (i) and (ii) above. The addition or subtraction of a constant, such as this one, to $\tilde{\phi}$ has no effect on boundary condition (iii) so we can write Equation (44) as

$$\tilde{\phi}(\eta,0) = -\frac{u_o^2}{2}e^{-2jk} - \sqrt{\frac{1-\eta}{\eta}}\left\{B(k) + \frac{u_o^2}{2\pi}\left[\int_0^\infty e^{-2jkt^2}\sqrt{\frac{t}{t+1}}\,\frac{dt}{t+\eta} - \int_1^\infty e^{-2jkt^2}\sqrt{\frac{t}{t-1}}\,\frac{dt}{t-\eta}\right]\right\}. \tag{45}$$

Equation (45) can be used to calculate the lift and moment on the profile. These follow from Equation (17b) which is now written as

$$\tilde{C}_p = -2\sqrt{\frac{1-\eta}{\eta}}\left\{B(k) + \frac{u_o^2}{2\pi}\left[\int_0^\infty e^{-2jkt^2}\sqrt{\frac{t}{t+1}}\,\frac{dt}{t+\eta} - \int_1^\infty e^{-2jkt^2}\sqrt{\frac{t}{t-1}}\,\frac{dt}{t-\eta}\right]\right\} \quad . \tag{46}$$

In terms of the present notation $\eta^2 = x/s$; and one can write

$$\tilde{C}_\ell = 2\int_0^1 \tilde{C}_p(\eta,0)\eta\,d\eta \quad ,$$

and

$$\tilde{C}_m = -2\int_0^1 \tilde{C}_p(\eta,0)\eta^3 d\eta \quad . \tag{47}$$

In the second of equations (47) the moment is measured about the nose of the profile and is taken as positive in the direction of α increasing. The use of Equation (46) in Equations (47) leads to a number of integrations which can be obtained in closed form. For example, those involving B(k) are among these. In other instances one interchanges the order of integration in Equations (47) and finally obtains

$$\tilde{C}_\ell = \frac{\pi}{2} B(k) + u_o^2 \left(\frac{1-e^{-2jk}}{2jk}\right) + 2u_o \left\{ \int_0^\infty e^{-2jkt^2} \left[\sqrt{t(t+1)} - \frac{1}{2}\sqrt{\frac{t}{t+1}} \right] dt + \int_1^\infty e^{-2jkt^2} \left[\sqrt{t(t+1)} - \frac{1}{2}\sqrt{\frac{t}{t-1}} \right] dt \right\} \tag{48}$$

and

$$\tilde{C}_m = -\frac{5\pi}{32} B(k) - u_o^2 \left[\frac{e^{-2jk}-1}{4k^2} - \frac{e^{-2jk}}{2jk} \right] + 2u_o \left\{ \int_0^\infty e^{-2jk} \left[\frac{1}{16}\sqrt{\frac{t}{t+1}} + \left(\frac{3}{8} - \frac{t}{2} + t^2\right)\sqrt{t(t+1)} \right] dt - \int_0^\infty e^{-2jk} \left[\frac{1}{16}\sqrt{\frac{t}{t-1}} + \left(\frac{3}{8} + \frac{t}{2} + t^2\right)\sqrt{t(t-1)} \right] dt \right\} \quad . \tag{49}$$

It now remains to evaluate the coefficient B(k) by applying condition (iv) above. As a preliminary to this evaluation we note that having obtained Equation (45) we now know $\tilde{\phi}(\eta,0)$ everywhere on the real ν-axis. Moreover, $\tilde{\psi}(\eta,0) = B(k)$ on the wetted surface, $0 \le \eta \le 1$, but we have not as yet found it on other parts of the real ν-axis. However for our purposes it is necessary to find $\mathrm{Im}F(\nu)$ on the upper half of the imaginary ν-axis. This determination is facilitated if $F(\nu)$ is treated as the sum of two functions,

$$\tilde{F}(\nu) = \hat{F}(\nu) + H(\nu) \quad ,$$

where

$$\mathrm{Re}\hat{F}(\xi,0) = 0 \ , \ \xi \le -1 \ , \ \xi \ge 0 \qquad \text{(on the cavity)} \quad ,$$

$$\mathrm{Im}\hat{F}(\xi,0) = B(k) \ , \ -1 \le \xi \le 0 \qquad \text{(on the foil)} \quad ,$$

and where

$$\mathrm{ReH}(\xi,0) = -\frac{u_o^2}{2} e^{-2jk\xi^2} \quad , \ \xi \leq -1 \ , \ \xi \geq 0 \qquad \text{(on the cavity)} \ ,$$

$$\mathrm{ImH}(\xi,0) = 0 \ , \ -1 \leq \xi \leq 0 \qquad \text{(on the foil)} \ . \tag{50}$$

The boundary value problem for $\hat{F}$ has the same form as the first order steady flow problem treated previously. Therefore we can write down the analytic function $\hat{F}(\zeta)$ without further ado. Thus in the ζ and the ν-planes we have

$$\hat{F} = \frac{-2iB}{\zeta - 1} = -iB\left(1 - \sqrt{1 + \frac{1}{\nu}}\right) \ .$$

Then if one puts $\nu = i\eta$ for points on the upper half of the imaginary axis of the ν-plane, he can write

$$\tilde{\psi} = -B(k)\left[1 - \sqrt{\frac{1}{2}\left(\sqrt{1 + \frac{1}{\eta^2}} + 1\right)}\right] + \mathrm{ImH}(0,\eta) \ . \tag{51}$$

In order to find the function H we employ the transformation (41) and the Hilbert transform (42) to determine ImH on the real axis off the foil in the ν-plane. Then ImH is known everywhere on the real axis and its value on the upper half of the imaginary axis in the ν-plane can be obtained with the aid of the Poisson integral. In particular we find from (41) and (50) that

$$\mathrm{ReG} = \begin{cases} -\dfrac{u_o^2}{2}\sqrt{\dfrac{|\xi|}{1 - |\xi|}}\, e^{-2jk\xi^2} \ , & \xi < -1 \ ; \\ 0 \qquad\qquad\qquad\qquad & -1 \leq \xi \leq 0 \ ; \\ -\dfrac{u_o^2}{2}\sqrt{\dfrac{\xi}{\xi + 1}}\, e^{-2jk\xi^2} \ , & 0 < \xi \ . \end{cases}$$

Then it follows for $\xi = -q < -1$ that

$$\mathrm{ImH} = \frac{u_o^2}{2\pi}\sqrt{\frac{q-1}{q}}\left\{ P\int_1^\infty \sqrt{\frac{t}{t-1}}\,\frac{e^{-2jkt^2}}{q-t}\,dt + \int_o^\infty \sqrt{\frac{t}{t+1}}\,\frac{e^{-2jkt^2}}{q+t}\,dt \right\} \ .$$

Note that when $\xi = -1$ $(q=1)$ ImH = 0. Thus the Kutta condition is satisfied. For $\xi > 0$ one has

$$\mathrm{ImH} = \frac{u_o^2}{2\pi}\sqrt{\frac{\xi+1}{\xi}}\left\{-\int_1^\infty \sqrt{\frac{t}{t-1}}\,\frac{e^{-2jkt^2}}{\xi+t}\,dt + P\int_o^\infty \sqrt{\frac{t}{t+1}}\,\frac{e^{-2jkt^2}}{t-\xi}\,dt\right\} .$$

Now that ImH is specified all along the real axis we can use the Poisson integral,

$$\mathrm{ImH}(0,i\eta) = \frac{\eta}{\pi}\int_{-\infty}^{\infty}\frac{\mathrm{ImH}(\xi,0)}{\xi^2+\eta^2}\,d\xi \quad ,$$

to write

$$\mathrm{ImH}(0,i\eta) = \frac{u_o^2}{2\pi^2}\,\eta\left\{P\int_1^\infty \sqrt{\frac{t}{t-1}}\,e^{-2jkt^2}\int_1^\infty \sqrt{\frac{q-1}{q}}\,\frac{dqdt}{(q-t)(q^2+\eta^2)}\right.$$

$$+\int_o^\infty \sqrt{\frac{t}{t+1}}\,e^{-2jkt^2}\int_1^\infty \sqrt{\frac{q-1}{q}}\,\frac{dqdt}{(t+q)(q^2+\eta^2)} - \int_1^\infty \sqrt{\frac{t}{t-1}}\,e^{-2jkt^2}\int_o^\infty \sqrt{\frac{\xi+1}{\xi}}\,\frac{d\xi dt}{(t+\xi)(\xi^2+\eta^2)}$$

$$\left. + P\int_o^\infty \sqrt{\frac{t}{t+1}}\,e^{-2jkt^2}\int_o^\infty \sqrt{\frac{\xi+1}{\xi}}\,\frac{d\xi dt}{(t-\xi)(\xi^2+\eta^2)}\right\} . \qquad (52)$$

Therefore it follows from Equation (51) that the desired result is

$$\tilde{\psi}(0,i\eta) = -\,B(k)\left[1 - \sqrt{\frac{1}{2}\left(\sqrt{1+\frac{1}{\eta^2}}+1\right)}\right] + \mathrm{ImH}(0,i\eta) \quad .$$

One can transform this expression from the upper half of the imaginary ν-axis to the negative real axis in the z-plane by means of the relation $(x/s) = -\eta^2$. The arguments leading to Equation (29) apply here too so that condition (iv) of zero downwash $\tilde{v}_2$ on the foil becomes

$$0 = -\,B(k) + 2jk\,B(k)\int_o^\infty e^{-2jkt}\left[1 - \sqrt{\frac{1}{2}\left(\sqrt{1+\frac{1}{t}}+1\right)}\right]dt -$$

$$2jk\int_o^\infty e^{-2jkt}H(t,0)\,dt \quad .$$

As before we have changed the variable of integration from $-(x/s)$ to t and the limits of integration have also been altered to suit this change. The function $H(t,0)$ is as defined in Equation (52) with $i\eta \to (-x/s) \to t$ also. Evidentially the function $B(k)$ is defined by

$$B(k) = \frac{-2jk \int_0^\infty e^{-2jkt} H(t,0)\,dt}{1 + j(2k)I_1(2k)} \quad , \tag{53}$$

where the integral $I_1(2k)$ has been defined previously by Equation (30) or by $L(2k)$ in Equation (31). As it stands the integration in the numerator of Equation (53) involves triple integrals. However if one inverts the order of integration, the last integration can be written as

$$\int_0^\infty \frac{e^{-2jk\xi^2}\eta\,d\eta}{\xi^2+\eta^2} = \frac{e^{2jk\xi^2}}{2}\left[-Ci(2k\xi^2) + j\,Si(2k\xi^2) - j\,\frac{\pi}{2}\right] .$$

Therefore Equation (53) can be written as

$$\begin{aligned} B(k) = -2jk\left(\frac{u_o}{\pi}\right)^2 L(2k)\Bigg\{ & P\int_1^\infty \sqrt{\frac{t}{t-1}}\, e^{2jkt^2} \int_1^\infty \sqrt{\frac{q-1}{q}}\, \frac{e^{2jkq^2}\left[-Ci(2kq^2)+j\left(Si(2kq^2)-\frac{\pi}{2}\right)\right]}{q-t}\,dq\,dt \\ & + \int_0^\infty \sqrt{\frac{t}{t+1}}\, e^{-2jkt^2} \int_1^\infty \sqrt{\frac{q-1}{q}}\, \frac{e^{2jkq^2}\left[-Ci(2kq^2)+j\left(Si(2kq^2)-\frac{\pi}{2}\right)\right]}{q+t}\,dq\,dt \\ & - \int_1^\infty \sqrt{\frac{t}{t-1}}\, e^{-2jkt^2} \int_0^\infty \sqrt{\frac{\xi+1}{\xi}}\, \frac{e^{2jk\xi^2}\left[-Ci(2k\xi^2)+j\left(Si(2k\xi^2)-\frac{\pi}{2}\right)\right]}{t+\xi}\,d\xi\,dt \\ & + P\int_0^\infty \sqrt{\frac{t}{t-1}}\, e^{-2jkt^2} \int_0^\infty \sqrt{\frac{\xi+1}{\xi}}\, \frac{e^{2jk^2}\left[-Ci(2k\xi^2)+j\left(Si(2k\xi^2)-\frac{\pi}{2}\right)\right]}{t-\xi}\,d\xi\,dt \Bigg\} . \end{aligned} \tag{54}$$

Equation (54) can be used in Equations (48) and (49) to complete the determination of the nonsteady lift and moment resulting from the gust-cavity interaction for sinusoidal gusts. Once these quantities have been evaluated numerically the corresponding responses to a sharp-edged streamwise gust may also be determined for this part of the solution as was done before for the other part. These solutions can then be combined vectorially to give the total nonsteady response in terms of k and the ratio α/u_o for sinusoidal gusts. For sharp-edged gusts, curves similar to Figure 7 can be obtained for various values of α/u_o.

CONCLUSIONS AND RECOMMENDATIONS

The present study has shown that there is a cavity flow analog of the Horlock function of airfoil theory which gives the response of the profile to streamwise sinusoidal gusts. This nonsteady response function for flows at zero cavitation number has been evaluated numerically for the entire range of reduced frequencies for both lift and moment on the profile and these results have been used to derive the transient lift and moment on the profile after it encounters a sharp edged gust. It is found that the results computed can be ascribed mainly to the direct action of the streamwise velocity fluctuations upon the inclined wetted surface of the hydrofoil. This is the only effect found in airfoil theory.

It has been found theoretically that the cavity flow causes the hydrofoil to experience an added nonsteady effect which is not found in airfoil theory. This added reaction occurs at twice the frequency of the input frequency of the gust. This part of the solution has been determined explicitly in the present study. It is independent of attack angle whereas the part of the solution which was determined first depends on both gust amplitude and attack angle. Thus one can assign the cause of this new nonsteady effect to be primarily an interaction between the cavity and the gust. To date numerical analysis of this part of the theory has not been carried out.

The formulae which have been derived for this second part of the solution indicate that the numerical work for its evaluation will be rather elaborate. Once this work has been done the total response of the profile can be obtained as a vectorial combination of the two sets of data for various ratios of steady attack angle to gust amplitude over the range of reduced frequencies. For the total response to the sharp-edged gust, results for the two parts may be added.

The ability of an oscillating surface to extract energy from the flow depends critically upon the phase relationships between the nonsteady reactions and the oscillatory input. The amplitude of these nonsteady reactions need not be large because it is the stability of the response which is important. Therefore, it is essential to evaluate this second part of the solution in order to explore this important aspect of this new theory. It is conceivable that the effects discovered during the course of this study could be important for analyses of the structural dynamics of fully cavitating hydrofoils in a seaway. For these reasons it is recommended that upon completion of the present study the theory be extended to include free surface effects.

APPENDIX

NUMERICAL CALCULATIONS

As long as the reduced frequency is not too large, numerical evaluations for I_2 and I_3 as defined by Equations (34) and (35), can proceed by standard methods. For the present Simpson's rule integrations, k-values ranged from zero to twenty-five. This rather large range was selected in order to permit the most effective joining with results obtained by means of asymptotic expansions for reduced frequencies ranging from ten to infinity. It also permits a check on the validity of the numerical integrations.

It was found that computer time could be reduced if one uses the fact that

$I_2(0) = \pi/4$ and $I_3(0) = 5\pi/64$, for then one can write

$$\text{Re } I_2 = \frac{\pi}{4} + \int_0^1 \sqrt{\frac{1}{\sqrt{\eta}} - 1}\,(\cos k\eta - 1)\,d\eta\,, \quad \text{Im } I_2 = -\int_0^1 \sqrt{\frac{1}{\sqrt{\eta}} - 1}\,\sin k\eta d\eta\,,$$

and

$$\text{Re } I_3 = \frac{5\pi}{64} + \int_0^1 \sqrt{\eta^{3/2}(1 - \sqrt{\eta})}\,(\cos k - 1)\,d\eta\,, \quad \text{Im } I_3 = -\int_0^1 \sqrt{\eta^{3/2} - \sqrt{\eta})}\sin k\eta d\eta\,.$$

Moreover, because all four integrands above have branch points at both $\eta = 0$ and $\eta = 1$, it was found helpful to devise special finite difference integration formulas for use near these points. All integrations were carried out with extended precision. They also used an accuracy test to determine an appropriate interval size for each k-value and for each of the four integrals. In order to obtain values of P and Q, one must also have values of the function L(k). These numerical data were taken from the tabulation of Reference 12 and used in the expressions

$$P = L(k) + \frac{4}{\pi} I_2(k)$$

and

$$Q = L(k) + \frac{64}{5\pi} I_3(k) \quad .$$

For values of k ranging from ten to infinity, the method of steepest descent [16,17] was used to find asymptotic expansions for I_2 and I_3. As one might expect, a contribution to the value of these integrals is obtained from both branch points of the integrand. The path of integration as specified in terms of the real variable, η, between 0 and 1, corresponds to a level curve. The results obtained by this procedure are:

$$I_2(k) \sim \frac{\Gamma(3/4)}{(jk)^{3/4}} - \frac{\Gamma(5/4)}{2(jk)^{5/4}} - \frac{\Gamma(7/4)}{8(jk)^{7/4}} - \frac{\Gamma(9/4)}{16(jk)^{9/4}} - \frac{5\,\Gamma(11/4)}{128(jk)^{11/4}}$$

$$- j\,\frac{e^{-jk}}{\sqrt{2}} \left\{ \frac{\Gamma(3/2)}{(jk)^{3/2}} - \frac{3}{8}\,\frac{\Gamma(5/2)}{(jk)^{5/2}} + \frac{7}{32}\,\frac{\Gamma(7/2)}{(jk)^{7/2}} \right\}$$

and

$$I_3(k) \sim \frac{\Gamma(7/4)}{(jk)^{7/4}} - \frac{1}{2}\,\frac{\Gamma(9/4)}{(jk)^{9/4}} - \frac{1}{8}\,\frac{\Gamma(11/4)}{(jk)^{11/4}} - \frac{1}{16}\,\frac{\Gamma(13/4)}{(jk)^{13/4}}$$

$$- j \frac{e^{-jk}}{\sqrt{2}} \left\{ \frac{\Gamma(3/2)}{(jk)^{3/2}} + \frac{5}{8} \frac{\Gamma(5/2)}{(jk)^{5/2}} - \frac{17}{128} \frac{\Gamma(7/2)}{(jk)^{5/2}} \right\} .$$

In order to calculate the response function P(k) and Q(k), the preceding results must be supplemented by asymptotic values of the function L(k) as indicated in the above Equations for P and Q. These additional values can be calculated directly from the asymptotic expansion of the quantity $1 + jkI_1$ [13]. In order to obtain values which provided adequate accuracy, it seemed necessary to obtain more terms from the expansion of $1 + jkI_1$ than is provided in Reference 13. The required extension of the formula is

$$1 + jkI_1(k) \sim \frac{1}{\sqrt{2}} \left\{ \Gamma(3/4)\ (jk)^{1/4} + \frac{1}{2} \frac{\Gamma(5/4)}{(jk)^{1/4}} + \frac{1}{8} \frac{\Gamma(7/4)}{(jk)^{3/4}} - \frac{1}{16} \frac{\Gamma(9/4)}{(jk)^{5/4}} - \frac{5}{128} \frac{\Gamma(11/4)}{(jk)^{7/4}} \right\}$$

An additional term, $\frac{107}{256} \frac{\Gamma(13/4)}{(jk)^{7/4}}$, was also found in order to determine the best number of terms to retain in the expansion. It was found that this additional term would have reduced the accuracy of the calculations and that, for values of reduced frequency exceeding ten, little, if any, difference is found between L(k) values calculated from the expansion of $1 + jkI_1$, as shown above or with only the first four terms as originally given in Reference 13. However, it was found helpful to recompute all the coefficients of k in this formula to more decimal places.

A tabulation of all numerical results for the sinusoidal gust response is shown in Table 1. These values of the complex functions defined by Equations for P(k) and Q(k) are shown plotted against reduced frequency in Figures 8 and 9. It should be recalled in connection with these results that all moments and forces are referred to the nose of the foil and that the reduced frequency is based on the profile chord and not upon the half chord as is common in airfoil theory.

The indicial admittance functions corresponding to an encounter of the foil with a sharp-edged gust or unit step in chordwise disturbance velocity can be found by direct superposition [13,14]. For the lift response, one can write

$$A_\ell(\lambda) = \frac{2}{\pi} \int_0^\infty \mathrm{Re}\ \{P(k)\} \frac{\sin \lambda k}{k}\, dk \quad . \tag{38}$$

For the moment response one has

$$A_m(\lambda) = \frac{2}{\pi}\int_0^\infty \text{Re}\,\{Q(k)\}\,\frac{\sin\lambda k}{k}\,dk \quad . \tag{39}$$

In these formulae the quantity λ is the distance traveled in chords after the profile nose hits the gust. We have already noted that Re $\{P\} \to 2$ and Re $\{Q\} \to 2$ as $k \to 0$. Moreover, the behavior of both Re $\{P\}$ and Re $\{Q\}$ is dominated by Re $\{L(k)\}$ as $k \to \infty$. It has been found that

$$\text{Re}\,L \sim \frac{1.0662}{k^{1/4}} - \frac{.1633}{k^{3/4}} \quad .$$

Evidentally, Re $\{P\}$ and Re $\{Q\}$ behave well enough at infinity so that the Fourier transforms for A_ℓ and A_m converge and one can write them as:

$$\begin{Bmatrix} A_\ell \\ A_m \end{Bmatrix} = \frac{2}{\pi}\int_0^\infty \begin{Bmatrix} 2 - [2 - \text{Re}\,P] \\ 2 - [2 - \text{Re}\,Q] \end{Bmatrix} \frac{\sin\lambda k}{k}\,dk = 2 - \frac{2}{\pi}\int_0^\infty \begin{Bmatrix} 2 - \text{Re}\,P \\ 2 - \text{Re}\,Q \end{Bmatrix} \frac{\sin\lambda k}{k}\,dk \quad .$$

This transformation takes care of the integrands at the origin so that asymptotic representations for these integrals as $\lambda \to \infty$ are easily obtained. It is necessary to approximate the quantities 2 - Re P and 2 - Re Q near k = 0 by suitable polynomials. From Table 1, it is found that

$$2 - \text{Re}\,P = .2050k \quad ,$$

$$2 - \text{Re}\,Q = .2025k + .1250k^2 \quad .$$

These forms appear to be consistent with the accuracy of the tabulated values. Now, it is known [18] that if F(x) and all of its derivatives exist as ordinary functions for $x \geq 0$, and are well behaved at infinity, then the asymptotic expansion of the Fourier transform of F is

$$\int_0^\infty F(x)\,\sin 2\pi xy\,dx \sim \frac{F(0)}{2\pi y} - \frac{F''(0)}{(2\pi y)^3} + \frac{F^{iv}(0)}{(2\pi y)^5} - \cdots \quad .$$

In order to apply this result to the present problem, we put

$$F(0) = \frac{2 - \text{Re}\,P}{k} = .2050 \text{ or } F(0) = \frac{2 - \text{Re}\,Q}{k} = .2025$$

and $\lambda = 2\pi y$. Thus, one has

$$A_{\ell}(\lambda) \sim 2 - \frac{2}{\pi}\left(\frac{.2050}{\lambda}\right) + 0\left(\frac{1}{\lambda^3}\right) \quad ,$$

and

$$A_{m}(\lambda) \sim 2 - \frac{2}{\pi}\left(\frac{.2025}{\lambda}\right) + 0\left(\frac{1}{\lambda^3}\right)$$

These expansions are used to supplement numerical integrations which are based upon the values of Table I and the asymptotic expansions

$$\text{Re } P \sim \frac{1.0662}{k^{1/4}} + \frac{.43373}{k^{3/4}} + 0\left(\frac{1}{k^{7/4}}\right) \quad ,$$

and

$$\text{Re } Q \sim \frac{1.0662}{k^{1/4}} - \frac{.16334}{k^{3/4}} + 0\left(\frac{1}{k^{7/4}}\right) \quad .$$

Results of such calculations for $A_{\ell}(\lambda)$ and $A_{m}(\lambda)$ are presented in Table II. Graphs of A_{ℓ} and A_{m} are shown in Figure 7.

REFERENCES

1. Thompson, D. E., "Measurement of Time-Dependent Propeller Thrust and Correlation with Theory," ORL TM 72-116, July 10, 1972.

2. Thompson, D. E., "Effects of Chordwise Velocity Variations in the Time-Dependent Thrust Generated by a Propeller Operating in a Spatially Varying Velocity Field," ARL TM 73-34, March 8, 1973.

3. Henderson, R. E. and H. Daneshyar, "Theoretical Analysis of Fluctuating Lift on the Rotor of an Axial Turbomachine," ARC R&M No. 3684, Her Majesty's Stationery Office, London, 1972.

4. Henderson, R. E., "The Upstream Unsteady Response of an Axial Flow Turbomachine to an Upstream Disturbance," Ph.D. Thesis, Department of Engineering, University of Cambridge, England, 1973.

5. Horlock, J. H., "Fluctuating Lift Forces on Aerofoils Moving Through Transverse and Chordwise Gusts," Transactions of the ASME, Journal of Basic Engineering, Vol. 90D, No. 4, 1968, pp. 494-500.

6. Chen, C. F. and R. A. Wirtz, "Second-Order Theory for Flow Past Oscillating Foils," AIAA Journal, Vol. 6, No. 8, August 1968, pp. 1556.

7. Sears, W. R., "Some Aspects of Non-Stationary Airfoil Theory and Its Practical Application," Journal of the Aeronautical Sciences, Vol. 8, 1941, pp. 104-108.

8. Morfey, C. L., "Lift Fluctuations Associated with Unsteady Chordwise Flow Past an Airfoil," Transactions of the ASME, Journal of Basic Engineering, Vol. 92, September 1970, pp. 663-665.

9. Commerford, G. L. and F. O. Carta, "An Exploratory Investigation of the Unsteady Aerodynamic Response of a Two-Dimensional Airfoil at High Reduced Frequency," United Aircraft Research Laboratories Report UAR-J182, United Aircraft Corporation, East Hartford, Connecticut, July 14, 1970.

10. Chen, C. F., "Second-Order Supercavitating Hydrofoil Theory," Journal of Fluid Mechanics, Vol. 13, Part 3, 1962, pp. 321-332.

11. Martin, M., "Unsteady Lift and Moment on Fully Cavitating Hydrofoils at Zero Cavitation Number," Journal of Ship Research, Vol. 6, No. 1, June 1962, p. 15.

12. Parkin, B. R., "Numerical Data on Hydrofoil Response to Nonsteady Motions at Zero Cavitation Number," Journal of Ship Research, Vol. 6, No. 3, December 1962, p. 40.

13. Parkin, B. R., "Fully Cavitating Hydrofoils in Nonsteady Motion," The RAND Corporation Research Memorandum TM-1939, Santa Monica, California, July 1957, DDC Document No. AD133017.

14. Scanlan, R. H. and R. Rosenbaum, Introduction to the Study of Aircraft Vibration and Flutter, MacMillan Co., New York, 1951, pp. 401-403.

15. Tricomi , F. G., Integral Equations, Interscience Publishers, New York, 1957, p. 166, 167.

16. Copson, E. T., An Introduction to the Theory of Functions of a Complex Variable, Oxford University Press, 1935, pp. 218-223 and 330-331.

17. Erdelyi, A., Asymptotic Expansions, Dover Publications, New York, 1956, pp. 39-46.

18. Lighthill, M. J., Fourier Analysis and Generalized Functions, Cambridge University Press, 1960, p. 56.

June 4, 1974
BRP:lhm

TABLE I

STEADY SINUSOIDAL GUST RESPONSE AT ZERO CAVITATION NUMBER

REDUCED FREQUENCY	I2 LIFT INTEGRAL REAL	I2 LIFT INTEGRAL IMAGINARY	I3 MOMENT INTEGRAL REAL	I3 MOMENT INTEGRAL IMAGINARY	P(K) LIFT RESPONSE REAL	P(K) LIFT RESPONSE IMAGINARY	Q(K) MOMENT RESPONSE REAL	Q(K) MOMENT RESPONSE IMAGINARY
0.000	0.7853	0.0000	0.2454	0.0000	2.0000	0.0000	2.0000	0.0000
0.010	0.7853	-0.0024	0.2454	-0.0012	1.9979	-0.0103	1.9979	-0.0124
0.020	0.7853	-0.0048	0.2454	-0.0025	1.9959	-0.0189	1.9959	-0.0231
0.040	0.7852	-0.0097	0.2453	-0.0051	1.9918	-0.0342	1.9917	-0.0427
0.060	0.7851	-0.0146	0.2452	-0.0077	1.9877	-0.0483	1.9874	-0.0609
0.080	0.7849	-0.0195	0.2451	-0.0102	1.9835	-0.0614	1.9830	-0.0783
0.100	0.7847	-0.0244	0.2450	-0.0128	1.9793	-0.0738	1.9785	-0.0950
0.120	0.7844	-0.0293	0.2448	-0.0154	1.9752	-0.0857	1.9740	-0.1111
0.160	0.7837	-0.0391	0.2443	-0.0205	1.9668	-0.1082	1.9646	-0.1420
0.200	0.7828	-0.0489	0.2438	-0.0256	1.9584	-0.1295	1.9550	-0.1718
0.300	0.7796	-0.0732	0.2417	-0.0383	1.9373	-0.1785	1.9297	-0.2415
0.400	0.7751	-0.0972	0.2389	-0.0508	1.9159	-0.2231	1.9024	-0.3065
0.500	0.7694	-0.1209	0.2353	-0.0631	1.8941	-0.2647	1.8731	-0.3681
0.600	0.7625	-0.1442	0.2309	-0.0751	1.8719	-0.3037	1.8417	-0.4264
0.700	0.7544	-0.1670	0.2257	-0.0868	1.8489	-0.3407	1.8082	-0.4818
0.800	0.7451	-0.1893	0.2199	-0.0981	1.8254	-0.3757	1.7725	-0.5345
0.900	0.7348	-0.2110	0.2133	-0.1089	1.8012	-0.4091	1.7348	-0.5846
1.000	0.7234	-0.2319	0.2061	-0.1193	1.7762	-0.4408	1.6951	-0.6317
1.200	0.6975	-0.2716	0.1899	-0.1384	1.7243	-0.4995	1.6101	-0.7178
1.400	0.6681	-0.3077	0.1716	-0.1551	1.6699	-0.5519	1.5185	-0.7923
1.500	0.6522	-0.3244	0.1618	-0.1625	1.6416	-0.5759	1.4709	-0.8259
1.800	0.6006	-0.3683	0.1302	-0.1804	1.5543	-0.6381	1.3202	-0.9042
2.000	0.5636	-0.3921	0.1079	-0.1886	1.4944	-0.6717	1.2165	-0.9410
3.000	0.3706	-0.4439	-0.0016	-0.1853	1.1968	-0.7470	0.7180	-0.9370
4.000	0.2122	-0.4008	-0.0754	-0.1250	0.9571	-0.6957	0.3795	-0.6949
6.000	0.1082	-0.2328	-0.0621	0.0056	0.7711	-0.4826	0.3799	-0.1632
2.500	0.4667	-0.4318	0.0512	-0.1959	1.3427	-0.7282	0.9572	-0.9767
3.500	0.2837	-0.4316	-0.0452	-0.1600	1.0659	-0.7336	0.5203	-0.8388
4.500	0.1595	-0.3585	-0.0907	-0.0857	0.8744	-0.6427	0.3017	-0.5359
5.000	0.1262	-0.3124	-0.0916	-0.0480	0.8182	-0.5842	0.2840	-0.3822
5.500	0.1105	-0.2698	-0.0808	-0.0166	0.7856	-0.5287	0.3156	-0.2542
7.000	0.1237	-0.1923	-0.0193	0.0189	0.7698	-0.4301	0.5333	-0.1081
8.000	0.1358	-0.1882	0.0070	0.0021	0.7668	-0.4237	0.6225	-0.1755
9.000	0.1262	-0.1970	0.0067	-0.0200	0.7398	-0.4336	0.6066	-0.2644
ASYMPTOTIC VALUES								
10.	0.1006	-0.1962	-0.0096	-0.0276	0.6965	-0.4313	0.5288	-0.2943
15.	0.0792	-0.1344	0.0045	-0.0051	0.6200	-0.3457	0.5375	-0.1956
20.	0.0566	-0.1030	-0.0010	0.0042	0.5582	-0.2995	0.4818	-0.1519
25.	0.0414	-0.0906	-0.0065	0.0017	0.5143	-0.2786	0.4350	-0.1565
81.	0.0172	-0.0401	-0.0012	0.0000	0.3712	-0.1838	0.3442	-0.1331
400.	0.0053	-0.0124	0.0000	0.0000	0.2433	-0.1102	0.2384	-0.0947
625.	0.0038	-0.0089	0.0000	0.0000	0.2168	-0.0965	0.2120	-0.0853
1000.	0.0026	-0.0062	0.0000	0.0000	0.1920	-0.0843	0.1886	-0.0762
10000.	0.0004	-0.0011	0.0000	0.0000	0.1070	-0.0452	0.1064	-0.0437

June 4, 1974
BRP:lhm

TABLE II

RESPONSE TO SHARP EDGED GUST AT ZERO CAVITATION NUMBER

CHORDS TRAVELED	LIFT RESPONSE	MOMENT RESPONSE
0.00	0.0000	0.0000
0.10	0.9579	0.6721
0.20	1.2408	0.8276
0.40	1.5891	1.1054
0.60	1.8018	1.4267
0.80	1.8904	1.7141
1.00	1.8065	1.8219
1.50	1.9129	1.9140
2.00	1.9347	1.9355
3.00	1.9564	1.9570
4.00	1.9673	1.9677
5.00	1.9738	1.9742
6.00	1.9782	1.9785
7.00	1.9813	1.9815
8.00	1.9836	1.9838
9.00	1.9854	1.9856
10.00	1.9869	1.9871
11.00	1.9881	1.9882
12.00	1.9891	1.9892
13.00	1.9899	1.9900
14.00	1.9906	1.9907
15.00	1.9912	1.9914
16.00	1.9918	1.9919
17.00	1.9923	1.9924
18.00	1.9927	1.9928
19.00	1.9931	1.9932
20.00	1.9934	1.9935
21.00	1.9937	1.9938
22.00	1.9940	1.9941
23.00	1.9943	1.9943
24.00	1.9945	1.9946
25.00	1.9947	1.9948

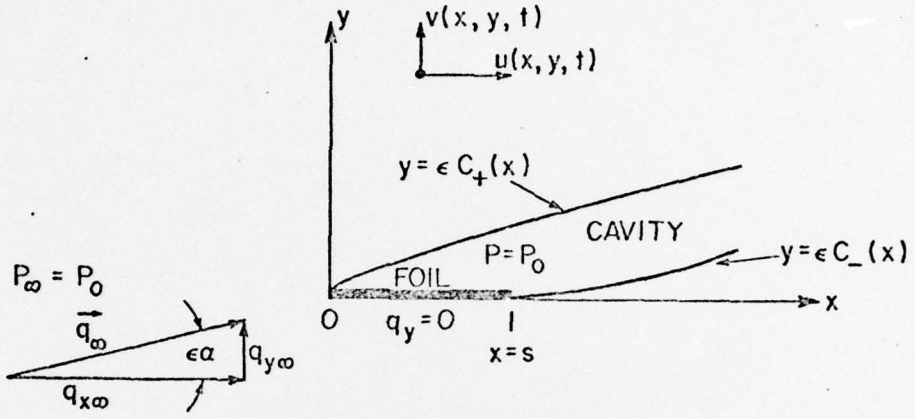

FIGURE 1 - Flow Geometry and Physical Quantities

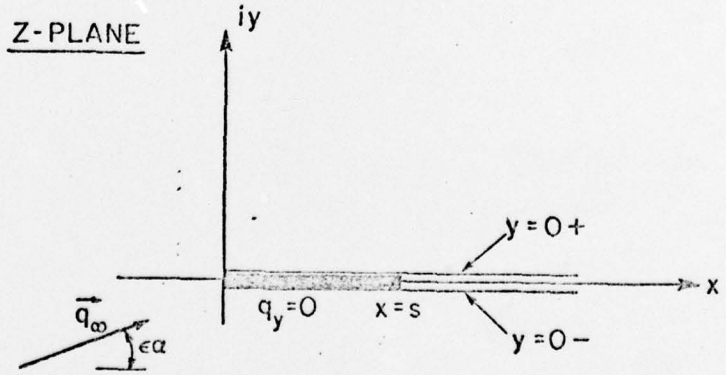

FIGURE 2 - Mathematical Representation of the Slender Body Approximation of the Cavity Flow

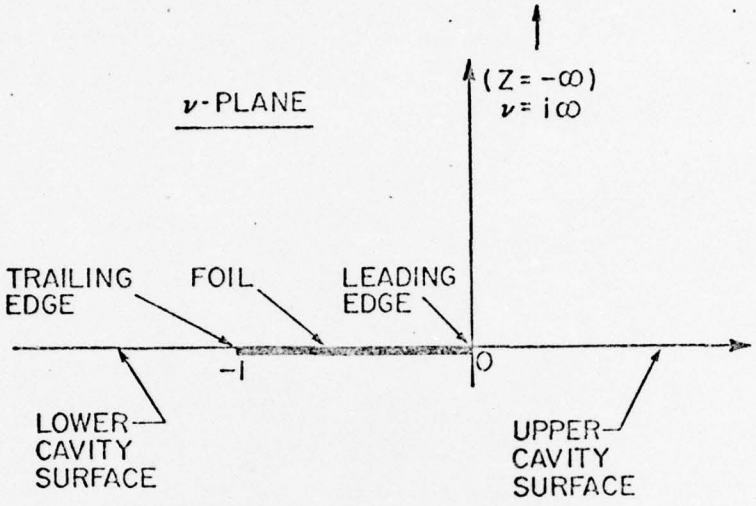

FIGURE 3 - Foil and Cavity in the ν-Plane

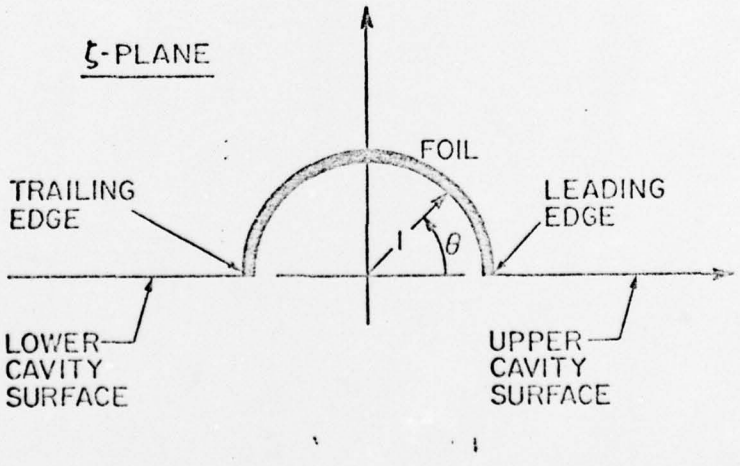

FIGURE 4 - Profile and Cavity in the ζ-Plane

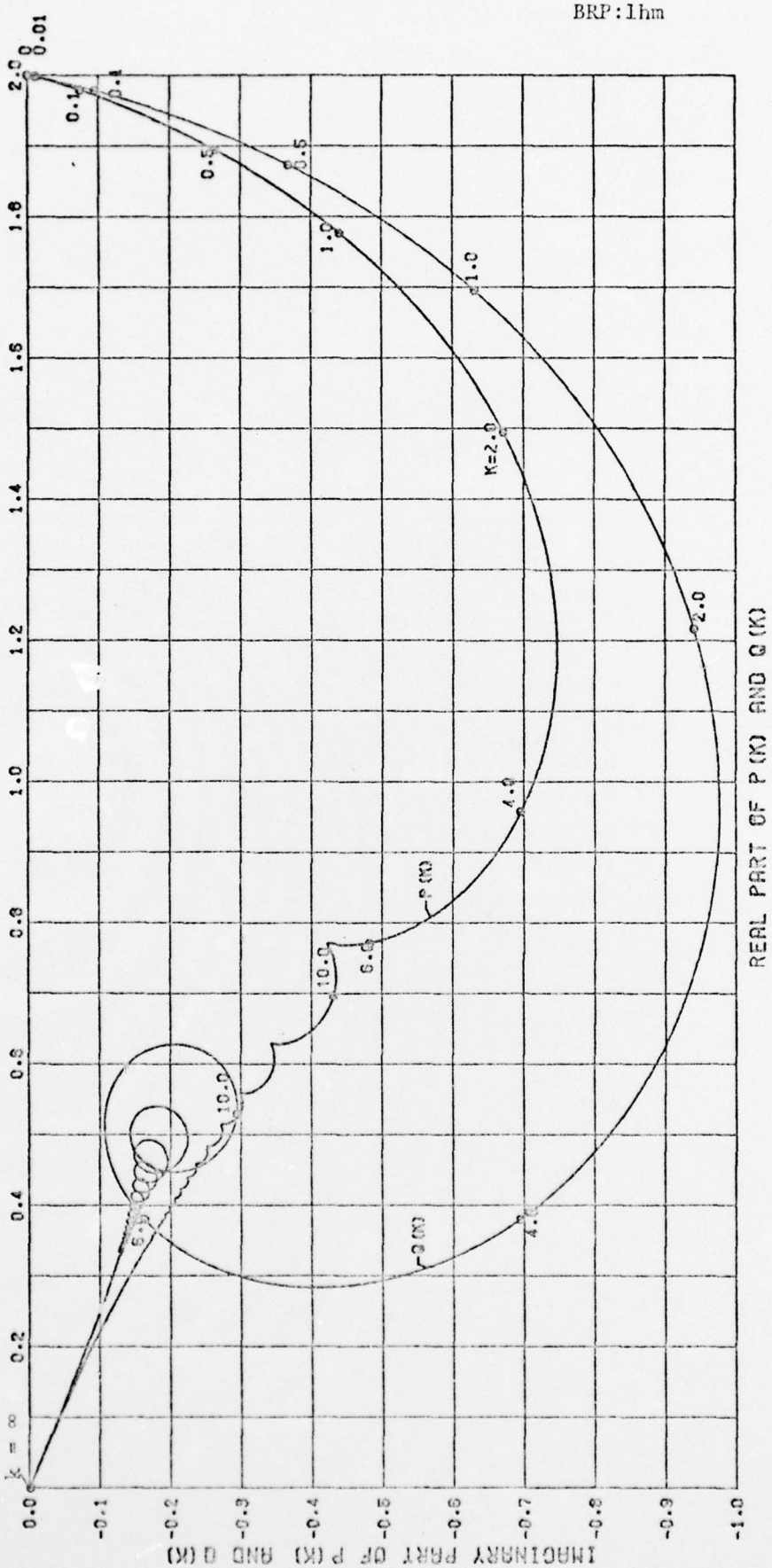

FIGURE 5 - Polar Plots of Lift and Moment Frequency Responses to Streamwise Sinusoidal Gusts for Flat Plate Hydrofoil at Zero Cavitation Number

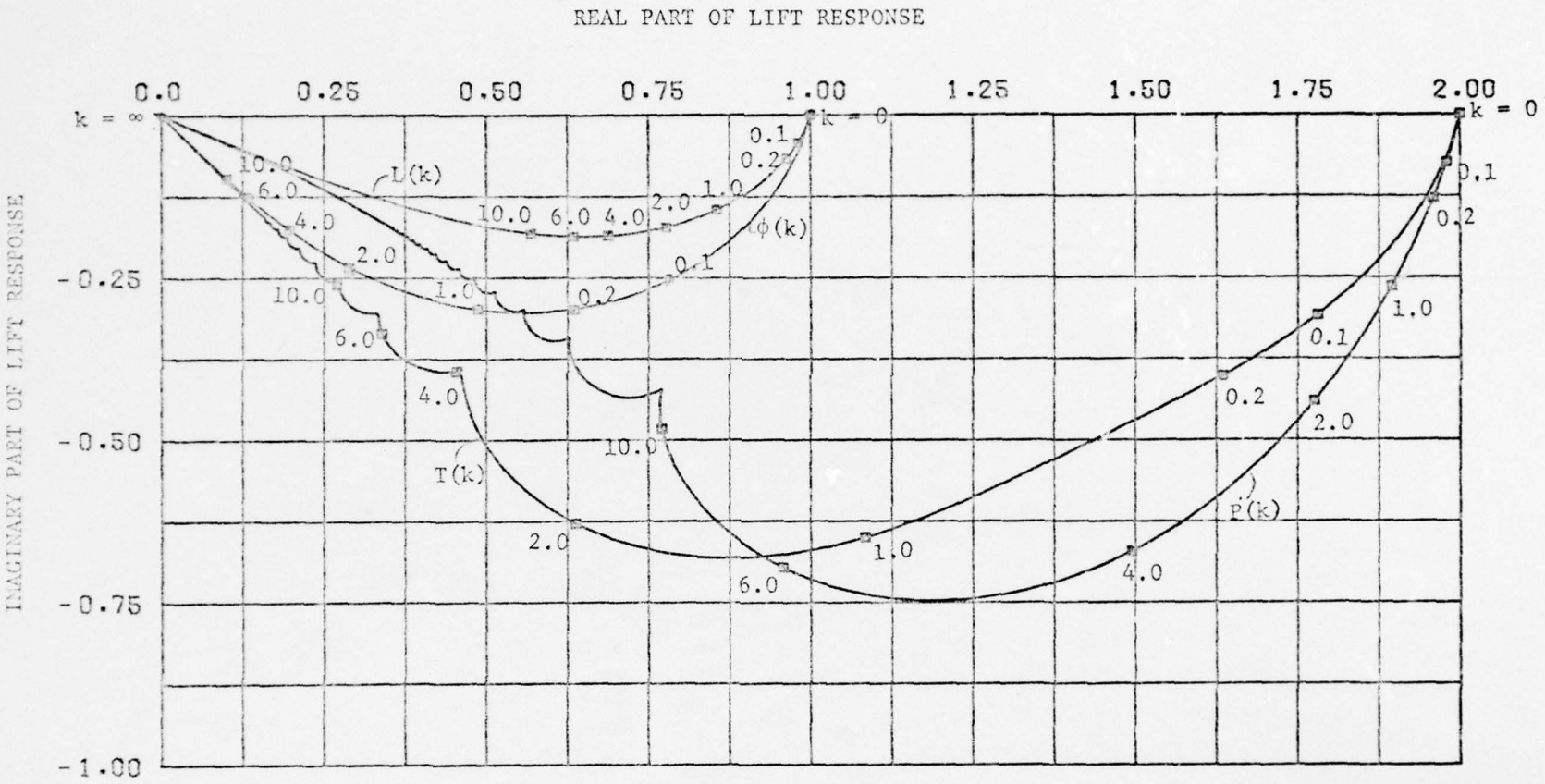

FIGURE 6 - Comparison of P(k) with the Horlock Function T(k), the Sears Function $\phi(k)$ and the Transverse Gust Function L(k). All Functions are Based Upon the Reduced frequency, $k = s\omega/U$, Referred to the Entire Profile Chord Length, s , with origin of Spatial Coordinates at the Profile Leading Edge. Cavitation number is zero for P and L.

June 4, 1974
BRP:lhm

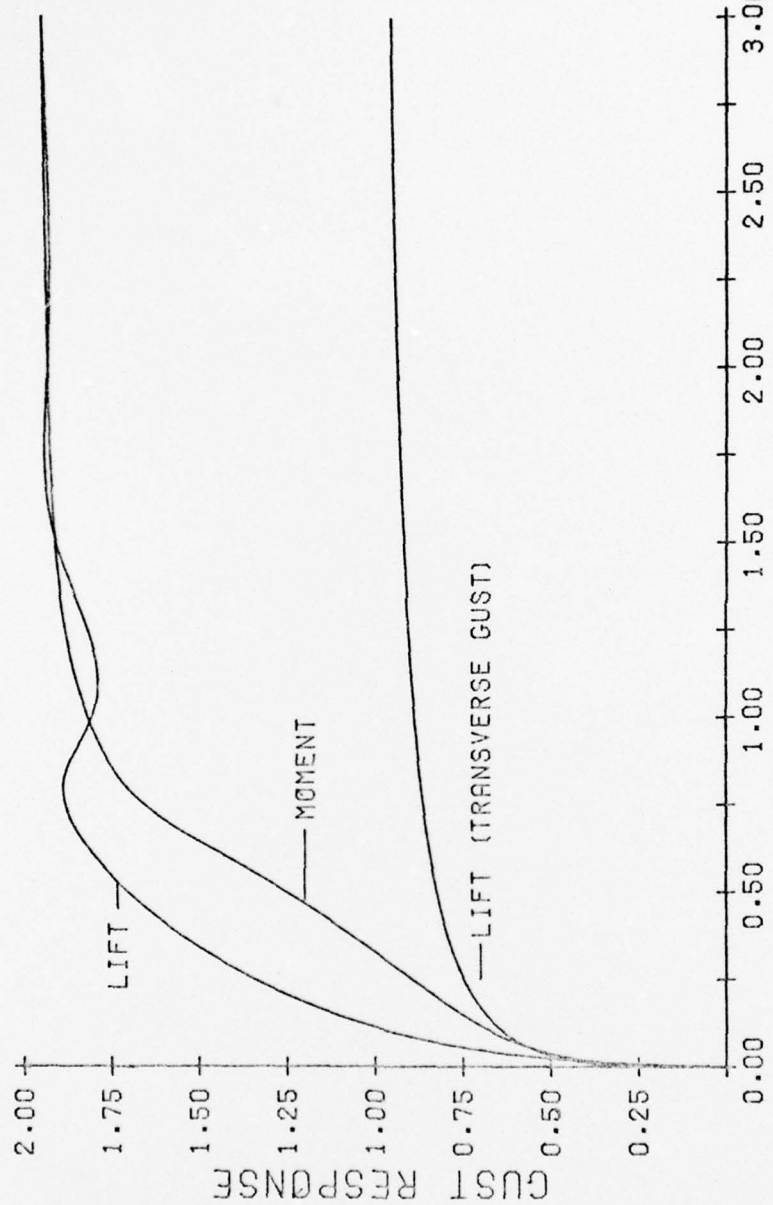

FIGURE 7 - Lift and Moment Build-up After An Encounter with a Sharp-Edged Streamwise Gust at Zero Cavitation Number. Also Shown is the Lift Response After an Encounter with a Sharp-Edged Transverse Gust [12].

June 4, 1974
BRP:lhm

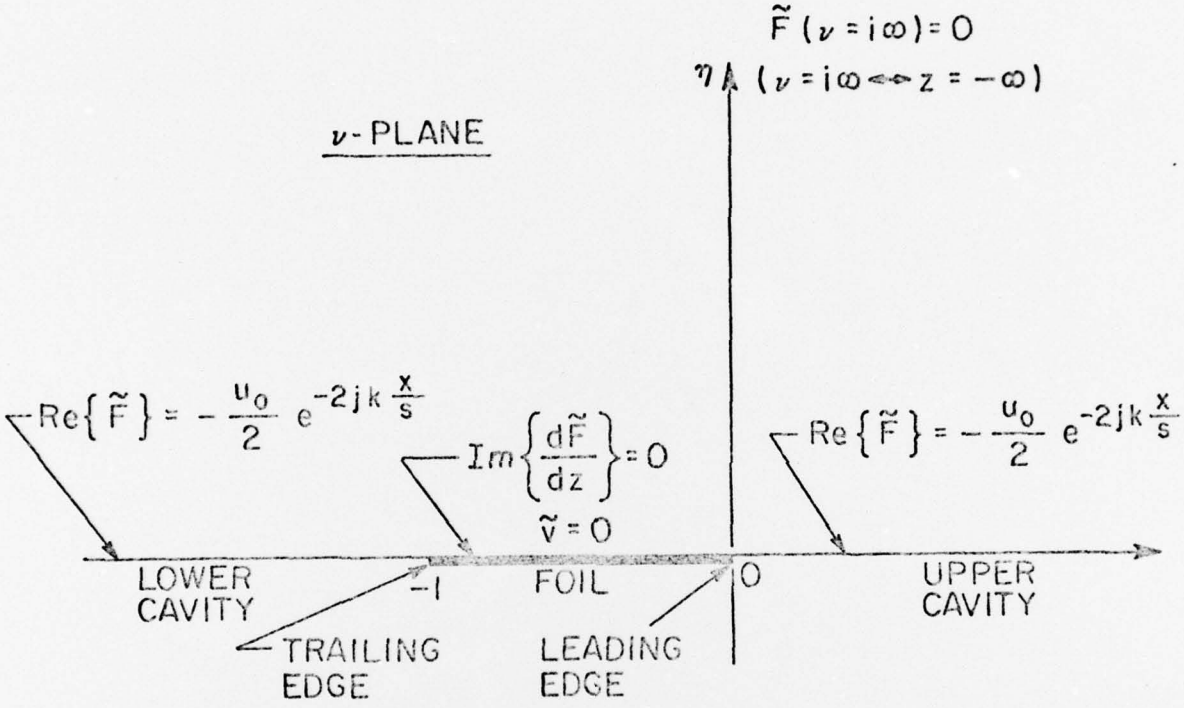

FIGURE 8 - The Mixed Boundary Value Problem for $\tilde{F}$ in the ν-Plane

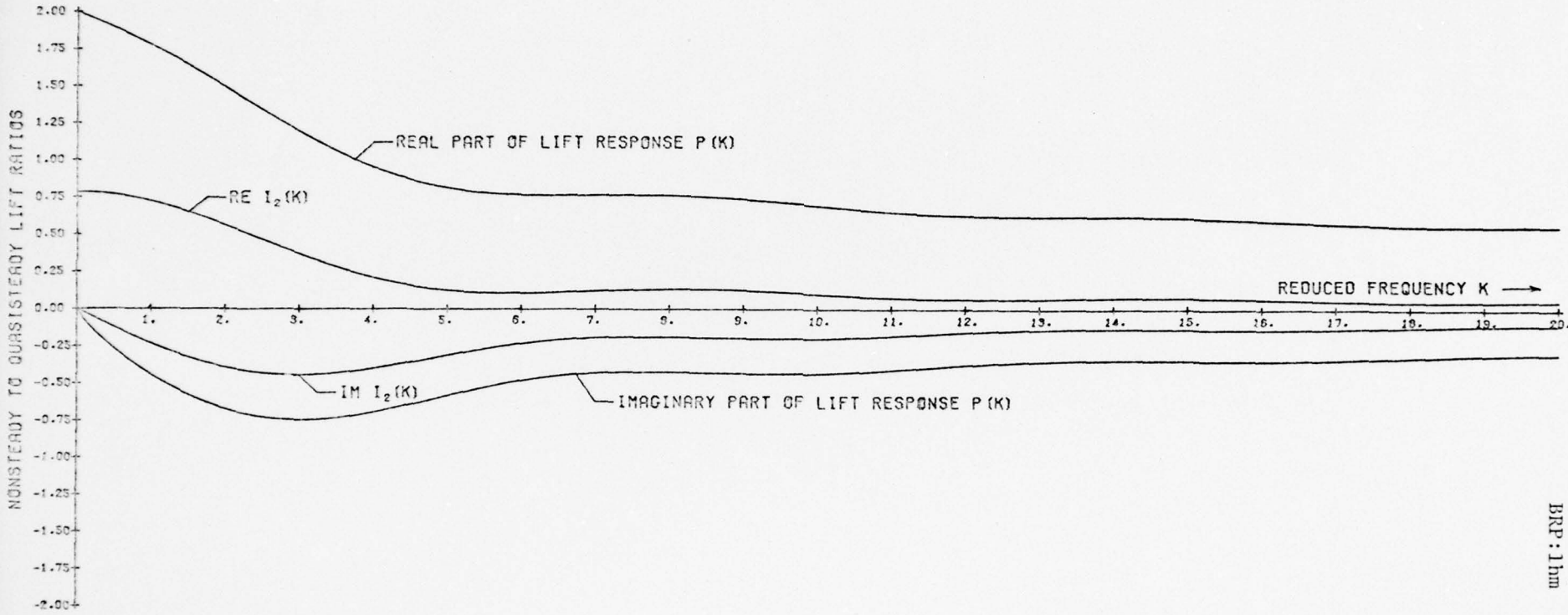

FIGURE 9 - Nonsteady Lift Versus Reduced Frequency for Steady Streamwise Sinusoidal Gusts Against a Flat Plate Hydrofoil at Zero Cavitation Number

June 4, 1974
BRP:lhm

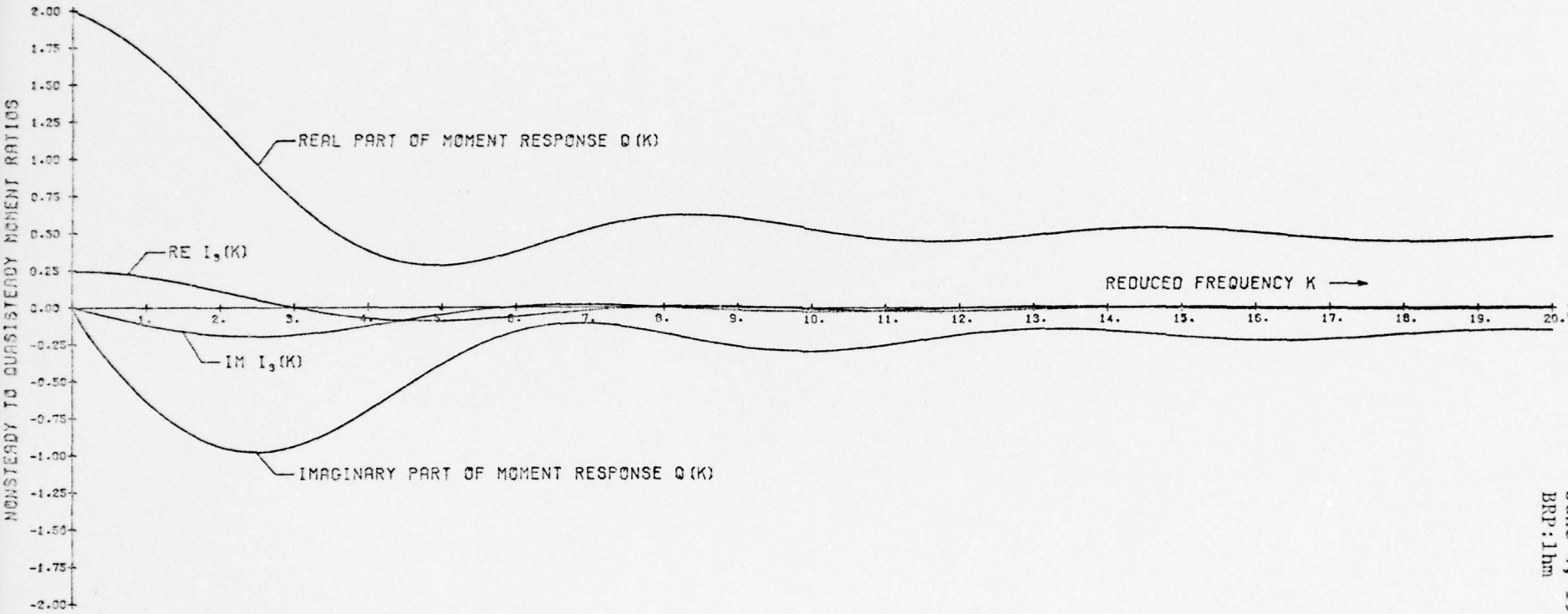

FIGURE 10 - Nonsteady Moment Versus Reduced Frequency for Steady Streamwise Sinusoidal Gusts Against a Flat Plate Hydrofoil at Zero Cavitation Number

June 4, 1974
BRP:lhm

Security Classification

DOCUMENT CONTROL DATA - R & D

(Security classification of title, body of abstract and indexing annotation must be entered when the overall report is classified)

1. ORIGINATING ACTIVITY *(Corporate author)*

Applied Research Laboratory
University Park, PA 16802

2a. REPORT SECURITY CLASSIFICATION
UNCLASSIFIED

2b. GROUP

3. REPORT TITLE

Fully Cavitating Hydrofoil Response to Streamwise Sinusoidal and Sharp-Edged Gusts at Zero Cavitation Number

4. DESCRIPTIVE NOTES *(Type of report and inclusive dates)*
Technical Memorandum

5. AUTHOR(S) *(First name, middle initial, last name)*

Blaine R. Parkin

6. REPORT DATE	7a. TOTAL NO. OF PAGES	7b. NO. OF REFS
June 4, 1974	43	18

8a. CONTRACT OR GRANT NO.	9a. ORIGINATOR'S REPORT NUMBER(S)
N00017-73-C-1418	TM 74-172
b. PROJECT NO.	
c.	9b. OTHER REPORT NO(S) *(Any other numbers that may be assigned this report)*
d.	

10. DISTRIBUTION STATEMENT

Approved for public release. Distribution unlimited.
Per NAVORD - Sept. 13, 1974.

11. SUPPLEMENTARY NOTES	12. SPONSORING MILITARY ACTIVITY
	Naval Ship Research and Development Center

13. ABSTRACT

A second-order linearized theory of two-dimensional cavity flows is used to study the nonsteady response of hydrofoil lift and moment to sinusoidal and sharp-edged streamwise gusts. These gust patterns are assumed to be frozen and to be convected at the steady free-stream velocity. The analysis is restricted to the case of zero cavitation number corresponding to an infinitely long cavity in an otherwise unbounded flow. For sinusoidal gusts, lift and moment response functions are presented for the entire range of reduced frequency. In addition, transient lift and moment responses are tabulated for the reactions which occur after the foil encounters a sharp-edged gust. These calculations are carried out for those terms in the solution which result from the nonsteady downwash on the wetted surface of the foil which are due to the direct action of the gust on the inclined wetted surface. They provide a direct cavity flow analog of the Horlock function of airfoil theory. The present study of a cavity flow has revealed an added nonsteady effect resulting from an interaction between the gust and the cavity. Theoretical results for this part of the solution are presented in this report which show a response at twice the input frequency of a sinusoidal gust. Numerical evaluation of this part of the theory has not been carried out.

DD FORM 1 NOV 65 1473 (PAGE 1) PLATE NO. 21856

S/N 0102-014-6600

Security Classification

14. KEY WORDS	LINK A		LINK B		LINK C	
	ROLE	WT	ROLE	WT	ROLE	WT
Convection	8					
Gust Patterns	8					
Hydrofoil	8					
Lift	8					
Moment	8					
Sharp-Edged Gusts	8					
Sinusoidal Gusts	8					
Streamwise Gusts	8					
Two-Dimensional Cavity Flow	8					
Zero Cavitation	8					

DISTRIBUTION LIST FOR UNCLASSIFIED TM 74-172 by B. R. Parkin (dated 4 June 1974)

Commander
Naval Sea Systems Command
Department of the Navy
Washington, DC 20360
Attn: Library
Code SEA-632
(Copies 1 and 2)

Naval Sea Systems Command
Attn: S. R. Marcus
Code SEA-03B
(Copy No. 3)

Naval Sea Systems Command
Attn: Code SEA-034B
(Copy No. 4)

Naval Sea Systems Command
Attn: T. E. Peirce
Code SEA-0351
(Copy No. 5)

Naval Sea Systems Command
Attn: G. R. Moltrup
Code SEA-54
(Copy No. 6)

Naval Sea Systems Command
Attn: Chief Technical Analyst
Code SEA-05121
(Copy No. 7)

Naval Sea Systems Command
Attn: Chief Analyst
J. J. Bellaschi
Code SEA-0313
(Copy No. 8)

Naval Sea Systems Command
Attn: A. R. Paladino
Code SEA-0372
(Copy No. 9)

Naval Sea Systems Command
Attn: Code SEA-03412
(Copy No. 10)

Naval Sea Systems Command
Attn: Code PMS-303
(Copy No. 11)

Commander
Naval Ship Engineering Center
Department of the Navy
Washington, DC 20360
Attn: W. L. Louis
Code 6136B
(Copy No. 12)

Naval Ship Engineering Center
Attn: R. M. Petros
Code 6148
(Copy No. 13)

Naval Ship Engineering Center
Attn: SEC-6110
(Copy No. 14)

Commanding Officer
Naval Underwater Systems Center
Newport, RI 02840
Attn: J. F. Brady
(Copy No. 15)

Naval Underwater Systems Center
Attn: J. D. Powers
(Copy No. 16)

Officer-in-Charge
Naval Undersea Center
San Diego Laboratory
San Diego, CA 92132
Attn: J. W. Hoyt
(Copy No. 17)

Naval Undersea Center
Attn: J. Green
(Copy No. 18)

Commanding Officer & Director
Naval Ship Res. & Dev. Center
Department of the Navy
Bethesda, MD 20034
Attn: Code 115
(Copy No. 19)

Naval Ship Res. & Dev. Center
Attn: Code 15
(Copy No. 20)

DISTRIBUTION LIST FOR UNCLASSIFIED TM 74-172 by B. R. Parkin (dated 4 June 1974)
CONTINUED

Naval Ship Res. & Dev. Center
Attn: Code 152
(Copy No. 21)

Naval Ship Res. & Dev. Center
Attn: Code 1524
(Copy No. 22)

Naval Ship Res. & Dev. Center
Attn: Code 1532
(Copies 23 and 24)

Naval Ship Res. & Dev. Center
Attn: Code 1542
(Copy No. 25)

Naval Ship Res. & Dev. Center
Attn: Code 1556
(Copies 26 and 27)

Naval Ship Res. & Dev. Center
Attn: Code 1572
(Copies 28 and 29)

Naval Ship Res. & Dev. Center
Attn: Code 1576
(Copy No. 30)

Commander
Naval Ordnance Laboratory
Silver Spring, MD 20910
Attn: Library
(Copy No. 31)

Dr. Allen J. Acosta
Prof. of Mechanical Engineering
Division of Engineering and Applied
Science
California Institute of Technology
Pasadena, CA 91109
(Copy No. 32)

Mr. T. F. Ogilvie
University of Michigan
Ann Arbor, MI 48105
(Copy No. 33)

Mr. C. T. Ray
Boeing Aerospace Company
Seattle, WA 98124
(Copies 34, 35, and 36)

Mr. H. R. Wright
Grumman Aircraft
Bethpage, Long Island, NY 11714
(Copy No. 37)

Defense Documentation Center
5010 Duke Street
Cameron Station
Alexandria, VA 22314

Via: Commander (SEA 632)
Naval Sea Systems Command
Department of the Navy
Washington, DC 20360
(Copies 38 - 49)

Dr. J. W. Holl
The Pennsylvania State University
Institute for Science & Engineering
Applied Research Laboratory
Post Office Box 30
State College, PA 16801
(Copy No. 50)

Dr. B. R. Parkin
The Pennsylvania State University
Institute for Science & Engineering
Applied Research Laboratory
Post Office Box 30
State College, PA 16801
(Copy No. 51)

Mr. G. B. Gurney
The Pennsylvania State University
Institute for Science & Engineering
Applied Research Laboratory
Post Office Box 30
State College, PA 16801
(Copy No. 52)

Dr. J. H. Kim
The Pennsylvania State University
Institute for Science & Engineering
Applied Research Laboratory
Post Office Box 30
State College, PA 16801
(Copy No. 53)

Mr. W. R. Hall
The Pennsylvania State University
Institute for Science & Engineering
Applied Research Laboratory
Post Office Box 30
State College, PA 16801
(Copy No. 54)

DISTRIBUTION LIST FOR UNCLASSIFIED TM 74-172 by B. R. Parkin (dated 4 June 1974)
CONTINUED

Mr. E. P. Bruce
The Pennsylvania State University
Institute for Science and Engineering
Applied Research Laboratory
Post Office Box 30
State College, PA 16801
(Copy No. 55)

Commanding Officer & Director
Naval Ship Res. & Dev. Center
Department of the Navy
Bethesda, MD 20034
Attn: W. B. Morgan
Code 526
(Copy No. 56)

Naval Ship Res. & Dev. Center
Attn: M. Strasberg
Code 901
(Copy No. 57)

Naval Ship Res. & Dev. Center
Attn: J. B. Hadler
Code 520
(Copy No. 58)

Naval Ship Res. & Dev. Center
Attn: M. Sevik
Code 019
(Copy No. 59)

Naval Ship Res. & Dev. Center
Attn: R. Wermter
Code 1520
(Copy No. 60)